PROCEEDINGS
OF THE
NATIONAL ACADEMY OF SCIENCES
Volume 26 March 15, 1940 Number 3
Copyright 1940 by the National Academy of Sciences

THE EXPERIMENTAL PRODUCTION OF MELANIN PIGMENT ON THE LOWER SURFACE OF SUMMER FLOUNDERS (PARALICHTHYS DENTATUS)[1, 2]

By Clinton M. Osborn

Department of Anatomy, Ohio State University

Communicated January 25, 1940

Differences in the degree of pigmentation on the upper and lower surfaces of animals have for centuries attracted man's interest. Such differential pigmentation, although perhaps most markedly exemplified in the lower vertebrates (fishes and amphibians), is seen also to a lesser extent in all the other vertebrate classes and even in many invertebrates.

Flounders provide an excellent example of differential pigmentation as they have entirely unpigmented lower sides but densely pigmented upper surfaces. They are doubly interesting because as larvae they display bilateral pigmentation which disappears on one side coincident with the migration of one eye and the secondary or adult orientation of the fish in a plane at right angles to the original (Agassiz, 1878). Naturally enough, Cunningham (1891, 1893, 1895) associated light with the presence of pigmentation and, on this basis, illuminated larval flatfishes ventrally to see if the bilaterally pigmented pattern would be retained even after the metamorphosis of the fish and the secondary orientation of the body with one flat surface against the substrate. Although he failed to retain the original bilateral pattern, it was found in a fair percentage of cases that after several months of ventral illumination some pigment did develop on the normally unpigmented lower side. However, Agassiz (1878) reported no development of ventral[3] pigment in flounder larvae which were exposed to light ventrally for the express purpose of arresting the migration of the eye in metamorphosis.

[1] This work was aided in part by a Bache Fund grant administered by Professor G. H. Parker.

[2] Contribution No. 247 of the Woods Hole Oceanographic Institution whose research facilities were generously provided for this investigation.

[3] The term "ventral" will be used in this paper to indicate the lower surface of a naturally oriented fish.

This paper presents descriptive data on preliminary experiments designed to show the relationship between directed continuous illumination, vision and the production of melanin pigment.

Materials and Methods.—The experimental flatfishes, summer flounders (*Paralichthys dentatus*) 11 to 17 inches long, were taken by otter trawl from Woods Hole waters. Live cars of neutral shade were anchored in the harbor for storing stock animals but most of the fishes used were freshly

FIG. A, EXPERIMENTAL SETUP PROVIDING VENTRAL ILLUMINATION

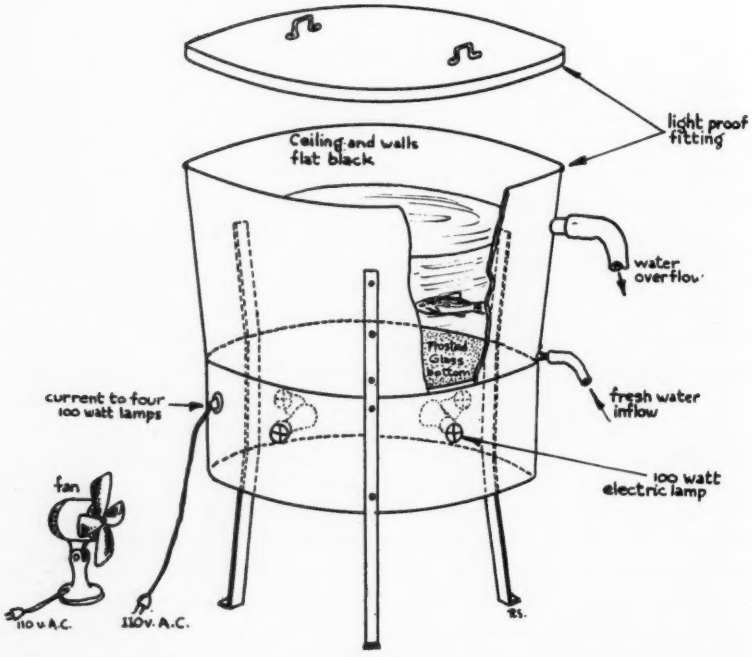

netted. Ventral illumination was provided by an apparatus similar to that shown in Fig. *A*. The temperature of the running sea water averaged 19°C. throughout these experiments. Some of the fishes were blinded by complete optic enucleation and in others both optic nerves were cut. Large experimental tanks painted black or white inside and illuminated continuously from above were used for extreme (black or white) back-

ground adaptation. Numerous controls were kept for each experimental situation.

Experiments and Observations:

1. *Unoperated Flounders with Lower Surface Illuminated.*—Eight freshly caught summer flounders were, on different occasions, placed in the apparatus providing a diffuse direct illumination of the lower side for periods ranging from seven to 51 days. Pigment developed to some extent on the normally pale surface (Fig. 1) of all of these fishes. In one flounder the first pigment was apparent after seven days but only after 15 to 25 days of ventral illumination was a melanin development obvious in most of the animals. After these initial stages the macroscopic increase in melanin was more rapid. A growth comparable to that in figures 2 and 3 was attained in about seven weeks. The general body shade (upper surface) of animals kept in the apparatus (black side walls and ceiling) was definitely darker than intermediate but yet not fully black-adapted. They were more nearly dark brown than black. Paler contrasty spots were frequently observed.

2. *Blinded Black Flounders Illuminated on Lower Surface.*—Five black-adapted flounders were blinded and placed in the apparatus providing ventral illumination. All of these fishes developed ventral pigment which first became apparent in 12 to 14 days and became pronounced in 45 days.

3. *Unoperated Flounders on Black Background Illuminated from Above.*—Another set of 12 unoperated fishes was placed in an experimental tank illuminated from above. The floor and side walls were flat black and the light source was of the same intensity as in the previous experiments. The animals became black-adapted in a few hours (Osborn '39*a*), finally reaching a fully black shade which persisted throughout the experiment. Typical white excitement spots could be elicited at any time upon application of the appropriate stimulus (Osborn '39*a*). The fishes remained in this situation for periods ranging from 15 to 70 days but none developed ventral pigment.

4. *Blinded Black Flounders on Black Background Illuminated from Above.*—Experiment 3 was repeated with ten flounders but this time the animals were totally blinded as soon as they were fully black-adapted. Such fishes were maintained under these conditions as long as 56 days but ventral pigment did not develop.

5. *Blinded Black Flounders on White Background Illuminated from Above.*—Summer flounders, 14 in all, were totally blinded following black-adaptation and were then transferred to white experimental tanks continuously illuminated from above. Flounders thus prepared remain maximally dark even on the white background (Osborn '39*a*). The light source was of the same intensity as employed above but the resulting illumination much brighter due to the high incidence of reflection from the

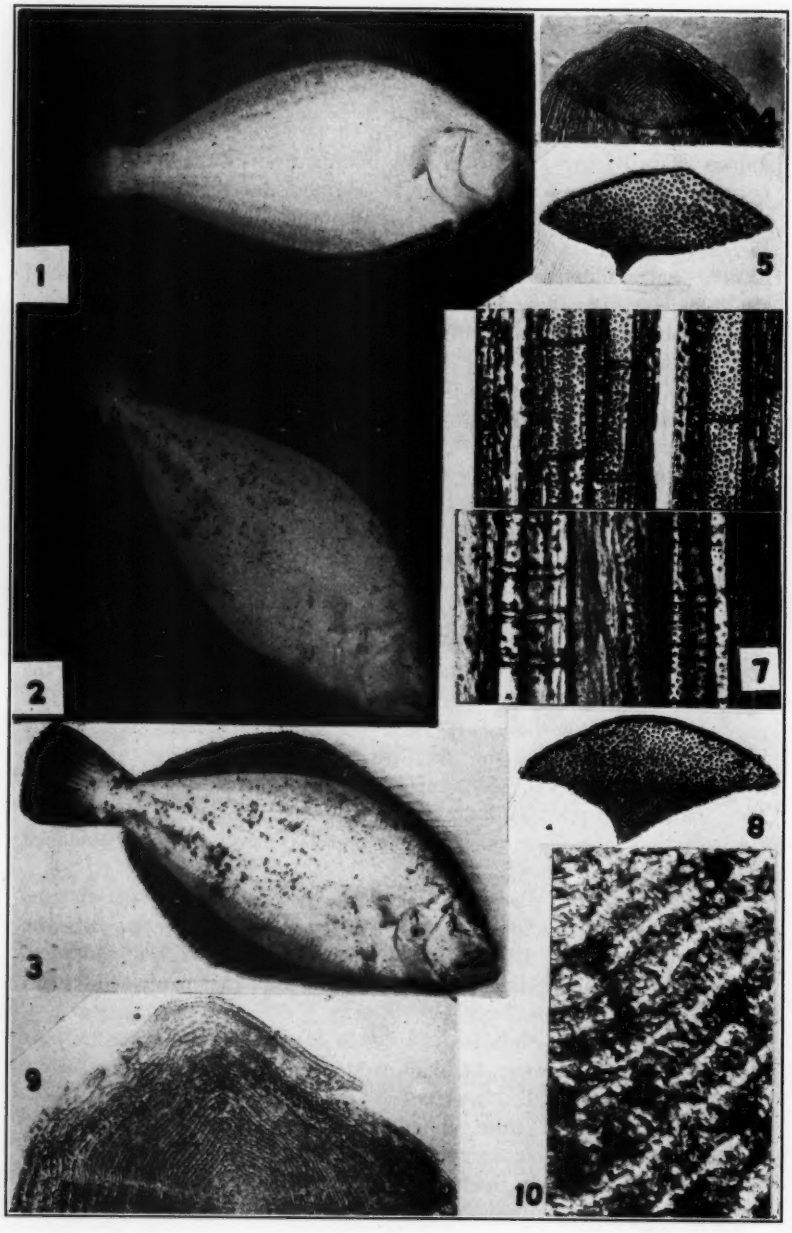
1
2
3
4
5
7
8
9
10

white floor and walls of the tank. Under these conditions, some evidence of developing ventral pigment appeared as soon as 15 days but the process was very slow and only a small amount developed in 60 to 70 days. Longer periods of treatment would undoubtedly result in increased pigmentation. However, the unmistakable amounts of ventral pigment developing in every fish suggest that vision is not essential to this process. On the contrary, normal unoperated control fishes placed under similar conditions at the same time failed to develop any ventral pigment and, of course, became typically white-adapted on the upper surface (Osborn '39*a*). Furthermore, it has been shown in fundulus and catfish that prolonged white-adaptation actually results in melanophore degeneration and an absolute decrease in the melanin of the skin (Odiorne '37).

6. *Blinded White Flounders on White Background Illuminated from Above.*—Nine fishes were completely white-adapted (seven days) and then totally blinded and replaced in illuminated white tanks under conditions identical with those of experiment No. 5. Summer flounders so prepared do not darken quickly and maximally as do many fishes but rather darken very slowly to an intermediate shade (Osborn '39*a* and *b*). Of nine such animals, six failed to develop appreciable amounts of ventral pigment in 40

PLATE 1

EXPLANATION OF FIGURES

Figure 1. Lower unpigmented surface of a normal summer flounder which was removed from nature and photographed immediately. The upper surface was in the dark phase. 1/5 natural size.

Figure 2. Lower surface of a summer flounder which had been illuminated ventrally for seven weeks in the apparatus in figure A. Note that considerable pigment has developed. 1/5 natural size.

Figure 3. Same as figure 2 but on white background to show the developed pigment in better contrast.

Figure 4. Photomicrograph of the exposed surface of a typical scale plucked from the lower surface of a normal untreated fish. Note that no trace of pigmentation is apparent. × 25.

Figure 5. Scale plucked from upper normally pigmented surface of a summer flounder. The scale surface is quite fully covered by melanophores. × 25.

Figure 6. Portion of the pectoral fin taken from the pigmented side of a control fish. It is highly pigmented. × 25.

Figure 7. Portion of the pectoral fin removed from the lower normally unpigmented surface of a fish which received ventral illumination for 6 weeks. This treatment has produced marked pigmentation. × 25.

Figure 8. A scale plucked from the lower surface of a fish illuminated ventrally 7 weeks. Note that it is pigmented as fully as is the dorsal scale in figure 5. × 25.

Figure 9. A scale from the lower surface of a fish illuminated ventrally for 3 weeks. Macroscopically only initial traces of pigmentation could be detected. Note that the melanophores are sparsely distributed. × 25.

Figure 10 An area of the scale in figure 9 showing the details of the newly developed melanophores. × 140.

to 50 days. The other three fishes exhibited early stages of melanophore development on a few scales. This experiment must be repeated on more animals and be allowed to run three or four months.

7. *Blinded Flounders on Illuminated Backgrounds.*—Seven summer flounders were totally blinded as soon as they were taken from nature. They were an intermediate greenish brown at the time. After blinding, they darkened slightly to a very homogeneous deep chocolate-brown and were placed in an illuminated *white* experimental tank as in the previous experiments. These fishes developed appreciable ventral pigment in 38 days and definitely more in 50 to 60 days. Two other fishes received similar treatment in all details but were placed in an illuminated *black* experimental tank. Pigment did not develop on the lower surface of either of these fishes in 52 days.

Discussion.—Perhaps Agassiz failed to get pigmentation because his light source (daylight) was not directed onto the lower surface of the fishes. They were simply placed in glass-bottomed dishes near the window. Since daylight varies in intensity with time of day and the weather, it would necessarily take two or three times as long for positive results as would continuous artificial illumination of constant high intensity. Agassiz, who was primarily interested in the migration of the eye in metamorphosis, probably did not continue his experiments long enough to grow pigment.

Cunningham designed his experiments for pigment studies, continued them for periods of from several months to over a year and reflected daylight by mirrors directly onto the lower surfaces of his fishes.

The confirmatory results presented here were obtained in relatively shorter periods probably because the light was of higher intensity and directed continuously onto the animals. These flounders were also larger and older than those used by previous investigators.

The artificially produced pigment is melanin in melanophores (Figs. 7, 8, 9 and 10) which appear to be normal morphologically and physiologically. When ventral scales bearing these melanophores are placed in adrenalin a typical concentration of the pigment granules occurs. Furthermore, when the scale is plucked and the nervous connections severed, the melanophores typically exhibit maximal expansion.

The source of these new melanophores is an unsettled question. Two possibilities are indicated: either they differentiate from some other cell already at the site or they migrate in from other areas. In the latter case they might migrate as typical melanophores or as cells capable of becoming melanophores. Experiments designed to provide more information on these points are now in progress. Thus far, no evidence for the migration of melanophores to the unpigmented area has been obtained. Cunningham, failing to find evidence to the contrary, believed that the pigment cells developed *in situ*.

Summary.—An apparatus providing continuous artificial illumination of constant intensity directed to the lower surface of flounders is pictured. Pigmentation was developed on the lower normally unpigmented surface in a high percentage of summer flounders in the following experimental situations: (1) Unoperated fishes in black tanks illuminated from below. (2) Blinded dark fishes in black tanks illuminated from below or in white tanks illuminated from above.

The observation that flounders blinded in the dark phase developed ventral pigment as readily as unoperated ones indicates that the eyes are not essential to this reaction.

Light is a necessary factor in the production of ventral pigment.

Agassiz, Alexander, "Development of the Flounders," *Proc. Amer. Acad. Arts Sci.*, **14** (1878).

Cunningham, J. T., "An Experiment Concerning the Absence of Color from the Lower Sides of Flatfishes," *Zoologischen Anzeiger*, **14**, 27–32 (1891), "Researches on the Coloration of the Skins of Flatfishes," *Jour. Mar. Biol. Assoc. United Kingdom*, **3** (new series), 111–118 (1893). "Additional Evidence on the Influence of Light in Producing Pigments on the Lower Sides of Flatfishes," *Ibid.*, **4**, 53–59 (1895).

Odiorne, J. M., "Morphological Color Changes in Fishes," *Jour. Exp. Zoöl.*, **73**, No. 3, 441–465 (1937).

Osborn, C. M., "The Physiology of Color Change in Flatfishes," *Jour. Exp. Zoöl.*, **81**, No. 3, 479–515 (1939*a*). "The Effects of Partial and Total Blinding on the Color Changes of the Summer Flounder (*Paralichthys dentatus*)," *Anat. Rec.*, **75**, abstract No. 242, p. 136 (1939*b*).

A RESPIRATORY PIGMENT FROM THE EGGS OF A MARINE WORM

BY N. H. HOROWITZ[1]

SCHOOL OF BIOLOGICAL SCIENCES, STANFORD UNIVERSITY

Communicated January 24, 1940

Of the wide diversity of pigments occurring in nature, a certain number are considered to function as respiratory carriers by virtue of their ability to be reversibly oxidized and reduced (see review of Barron[2]). I wish to report here the presence of such a pigment in the eggs of the marine worm *Urechis caupo*, together with evidence for its probable participation in cellular respiration.

The eggs of *Urechis caupo* are typically pink in color. In small, or relatively unripe, females, however, it is frequently found that the eggs are not pink, but yellow. Although the eggs of any one individual are all of the same color, a comparison of the eggs from different individuals shows

an intergradation of color from light yellow to an intense pink. It was found that if yellow eggs are placed in a Thunberg tube, and the tube then evacuated, they gradually become pink. If the vacuum is then broken and the eggs aerated, they regain their yellow color. The development of a pink color is apparently the result of the reversible reduction, *in vivo*, of a pigment present in yellow and pink eggs alike. The pigment in pink eggs can be oxidized by adding a small amount of H_2O_2 to the suspension (plus a trace of HCN to inhibit the powerful catalase contained in the cells). They thereupon become yellow. If the eggs are then washed and placed in an evacuated Thunberg tube they become pink again.

To obtain the pigment from the cells, pink eggs are extracted with acetone for 3–6 hours in a Soxhlet apparatus. This removes large quantities of two yellow pigments—one water-soluble and the other fat-soluble. The pink pigment remains behind. The nature of the two acetone-extractable pigments is as yet uncertain. Neither of them, however, shows reduction to a pink form. The pink pigment is then extracted by shaking with 5% HCl-methanol at 40°C. The pigment thus extracted consists of a mixture of the reduced form and its yellow oxidation product. If the extract is placed in the icebox overnight, the reduced form largely precipitates out in dark red, amorphous particles. The supernatant, containing the oxidized pigment and a small amount of the reduced pigment, is concentrated by distillation *in vacuo* and is finally dried on a water bath.

The oxidized form of the pigment is readily soluble in water. It is reduced by hydrosulfite, or by hydrogen in the presence of a platinum catalyst, to a pink (in concentrated solution, red) pigment. Upon shaking with air it reoxidizes to the yellow form. Autoxidation in air occurs rapidly at neutral and alkaline pH's. The reduced form is only sparingly soluble in acid solution ($<$pH 5.5). It is readily soluble at neutral and alkaline pH's, but immediately autoxidizes if oxygen is present. The pigment is rapidly destroyed by strong alkali. Autoxidation of the pigment can be accelerated *in vivo* by raising the intracellular pH by means of the penetrating base ammonia. Pink eggs so treated become yellow. Upon washing away the ammonia, the pink color returns.

The oxidation-reduction potential of the pigment has been determined polarographically[3] through the coöperation of Professor J. Percy Baumberger, using the purest preparation so far obtained. At pH 7.39 $E_0' = +0.163$ volt (250°C.). E_0' decreases 0.059 volt per unit increase in pH in the pH range 5–10. The change in E_h with change in degree of oxidation corresponds to a one-electron process. These results will be presented in detail in a future communication.

The facts that the pigment occurs naturally in both oxidized and reduced states, and that it is reducible by the cells and autoxidizes in the physiological range of pH, indicate that it is probably involved in the

cellular respiration. It is suggested that the pigment be called *urechrome* (not to be confused with the urinary pigment, urochrome). The chemical nature, absorption spectrum and physiological function of the substance are being studied.

[1] National Research Council Fellow in Zoölogy.
[2] Barron, E. S. G., *Physiol. Rev.*, **19**, 184–239 (1939).
[3] Müller, O. H., and Baumberger, J. P., *Trans. Electrochem. Soc.*, **71**, 169–194 (1937).

---

*FURTHER STUDIES ON THE PARTHENOGENETIC ACTIVATION OF RABBIT EGGS**

BY GREGORY PINCUS AND HERBERT SHAPIRO

PHYSIOLOGICAL LABORATORIES, CLARK UNIVERSITY, AND DEPARTMENT OF PHYSIOLOGY, VASSAR COLLEGE

Communicated February 8, 1940

In the course of certain studies on the artificial activation of rabbit tubal ova *in vitro* in which the development in culture of ova given certain stimulating treatments was contrasted with the development of untreated ova, we noted that in certain of the control cultures some ova gave clear evidence of activation. Our experiments were being conducted in a basement room at temperatures ranging between 17°C. and 21°C. Furthermore a period of one to two hours often elapsed between the sacrifice of the donor of the ova and their final incubation at 37.5°C. It seemed possible, therefore, that the cooling of rabbit ova might lead to activation. Some 80 unfertilized ova were cooled either by keeping them at room temperature for 2 to $3^1/_2$ hours (34 eggs) or by placing them in a refrigerator (at 6°C.) for 15 to 85 minutes (46 eggs). These ova, like all the others in our experimental series (see table 1), were cultured for 20 to 24 hours in rabbit serum at 37.5° (see Shapiro[3]), then fixed in Bouin's fluid (Pincus[1]), sectioned and stained with Ehrlich's hematoxylin, and examined for cytological evidences of activation.

In table 1 we present a summary of our data on the effects of cooling and also on the effects of exposing ova to: (1) balanced salt solutions made hypotonic by dilution with glass distilled water (usually 1 part salt solution to 1 part distilled water), (2) rabbit serum diluted to one-half by distilled water, (3) hypertonic balanced salt solutions (1.6 to 1.8% salt) and (4) hypertonic and hypotonic solutions alternately. Ova are considered activated when they exhibit clear pronuclei, or cleavage chromosomes, or cleavage. Ova classified as not activated either showed marginal meiotic

chromosomes (as at ovulation), or subnuclei (due to the scattering of meiotic chromosomes and nucleus reformation about single chromosomes or groups), or cytoplasmic fragmentation without cleavage. In some instances ova showed true cleavage had occurred followed or accompanied by cytoplasmic fragmentation—such eggs were considered activated.

The cooled ova appear to have been activated (and proceeded to cleavage) in a larger proportion than the other ova of these series. Actually our data indicate that cooling at 6°C. for 10 to 30 minutes was most effective: of 33 such ova 13 were activated and 10 cleaved, 7 of these cleavages without any cytoplasmic fragmentation. Of 13 ova placed at 6°C. for 85 minutes, 6 cleaved but 5 of these 6 showed cytoplasmic fragmentation.

We decided to attempt to cool ova *in situ* in the fallopian tubes. At 14 to 19 hours after the injection of an ovulating pituitary extract (Pincus[1, 2])

TABLE 1

THE EFFECTS OF VARIOUS TREATMENTS ON UNFERTILIZED RABBIT OVA CULTURED *in vitro* FOR 20 TO 24 HOURS

TREATMENT	NUMBER OF EGGS	NUMBER ACTIVATED	NUMBER CLEAVED	% ACTIVATED	% CLEAVED
Controls, no treatment	143	20	11	14.0	7.9
Cooling	80	42	19	52.5	23.8
Hypotonic balanced salt solutions	92	37	16	29.3	17.4
Hypotonic serum	354	134	32	37.9	9.0
Hypertonic balanced salt solutions	24	7	2	29.2	8.3
Alternating hypertonic and hypotonic solutions	29	9	2	31.0	7.0

the ovulated ova are massed below the first loop of the fallopian tube in a narrow portion and ordinarily so distend the tube as to be visible as a translucent bulge. We designed a hollow brass jacket which would enclose 3 centimeters of the tube at this point. Laparotomy was performed under combined ether and nembutal anesthesia, the sterilized cooling jacket placed about the right fallopian tube, and ice water circulated through the cooling jacket for appropriate periods of time.

Four females whose right fallopian tubes were so cooled for 15 minutes were sacrificed at various times after the operation. One killed on the second day after cooling showed a few ovulation points on each ovary, but only one uncleaved ovum was recovered from the cooled tube, none from the left (uncooled side). A second was killed at five days after cooling. Eight ova were recovered from the right oviducts of which one was a collapsed blastocyst, one a morula and the others fragmented or uncleaved. Two others sacrificed at 20 and 21 days, respectively, after the cooling operation

had neither eggs nor embryos, but one had a resorption site in the right uterus.

A number of other animals underwent the cooling operation and were allowed to go to term. The details are given in table 2.

TABLE 2

THE EFFECTS OF COOLING THE RIGHT FALLOPIAN TUBE CONTAINING FRESHLY OVULATED OVA

NUMBER OF RABBITS	PERIOD OF COOLING (MINUTES)	RESULT
1	5	No young
2	10	No young
7	15	No young
2	20	One gave birth to one living female
4	Frozen with solid CO_2 2 to 10 minutes	No young

Since these rabbits should have ovulated 12 to 15 ova on the operated side (Pincus[2]) it can be seen that one egg in over 200 developed into a living rabbit. This is less than would be expected if all the ova that presumably cleaved proceeded to develop normally. It has already been shown (Pincus[1]) that rabbit ova artificially activated by other methods may degenerate at any stage of development, and that the expectation of recovery of young is therefore very small.

Full details of these experiments will be published elsewhere.

* Aided by grants from the American Academy of Arts and Sciences and the American Philosophical Society.

[1] Pincus, G., *Jour. Exp. Zool.*, **82**, 85 (1939).

[2] Pincus, G., *Anat. Rec.* (in press).

[3] Shapiro, H., *Science*, **90**, 308 (1939).

GALACTIC AND EXTRAGALACTIC STUDIES, VI. SUMMARY OF A PHOTOMETRIC SURVEY OF 35,500 GALAXIES IN HIGH SOUTHERN LATITUDES

BY HARLOW SHAPLEY

HARVARD COLLEGE OBSERVATORY

Communicated February 12, 1940

1. Introduction.—The distribution of galaxies on the surface of the sky is easily examined on any uniform collection of long exposure photographs. But an effective study of the distribution in the line of sight requires much greater labor and is complicated by the serious difficulties of nebular photometry and uncertainties concerning the spread of intrinsic luminosity; for when we attempt to measure the space density of external galaxies, and its variation from place to place, it is necessary to use photometric methods for estimating distances. We must measure the apparent magnitudes as dependably as possible, adopt reasonable values of the space absorption and of the mean absolute magnitude and its dispersion, and survey large areas in order to diminish the effects of statistical fluctuations.

It is hoped that through the systematic photometry of large numbers of external galaxies, such as the one summarized in the present paper, it will be possible to trace the metagalactic gradients which have been shown in earlier communications[1] to affect the space density of galaxies within the easily explorable surrounding volume of space that has a radius of the order of a hundred million light years.

A considerable amount of work has already been done at the Harvard Observatory on the frequency of apparent magnitudes and on the immediately related question of space-density variations in the line of sight.[2] The present study, however, has the advantage over some earlier studies of referring only to areas in high latitude. It is not seriously troubled, therefore, by space absorption, unlike the situation in the earlier studies of 36,000 objects in the south celestial polar area (equatorial coördinate system), and of nearly 17,000 in the northern.

Approximately 31,500 galaxies have been measured for the determination of the magnitude frequencies that are summarized in table 2. All the fields lie in galactic latitudes between $-55°$ and the south galactic pole—a region that appears from examination of the distribution of faint stars on twenty 3-hour exposure, small-scale plates to be wholly free of irregularities in space absorption; it appears in fact, from earlier studies of the south galactic cap, to be entirely free of absorption of the sort that would produce a measurable latitude effect on the magnitudes of external galaxies. From the current study we should obtain, therefore, a very good value for the

mean space-density parameter,* defined by

$$m_1 = m - \frac{1}{b} \log \overline{N}, \qquad (1)$$

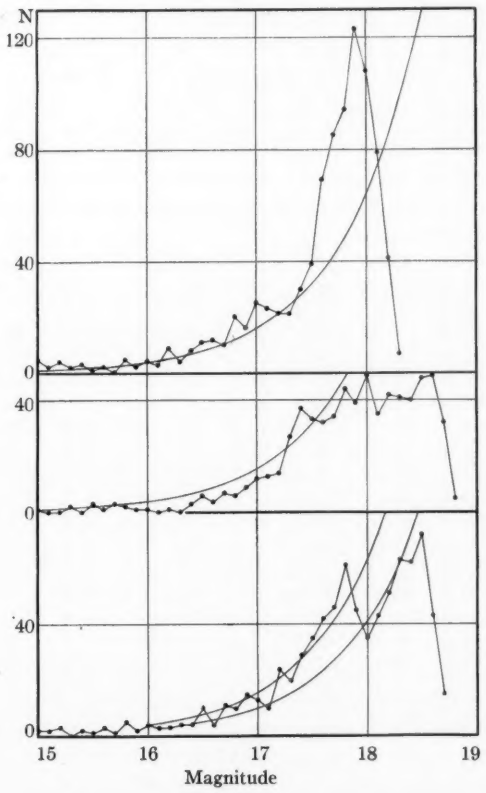

FIGURE 1

Frequency of magnitudes on plates *A* 20433 (top), 20503 and 20341. Ordinates are numbers in tenth-of-a-magnitude intervals; abscissae are observed photographic magnitudes.

which relates $\overline{N}$, the average number of nebulae (down to a given magnitude) per square degree, to that apparent magnitude m, on the assumption of uniform distribution (or linear density gradients) throughout space, and

* The symbol N_1 was inappropriately used for this parameter in the fourth paper of the current series. m_1 is obviously the value of m to which we must go to find one galaxy per square degree. For uniform space distribution the gradient b is 0.6.

general similarity in the luminosity function from place to place in the metagalaxy.

More than twenty individuals have taken part in this investigation, which has been in progress for several years. The marking of the galaxies on the Bruce plates was done chiefly by Mrs. S. F. M. Lindsay, Miss Constance Boyd and Miss Frances Wright. Miss Boyd and Miss Wright have independently estimated the magnitudes. Mr. Robert Porter and Miss Edith Jones made many of the star counts for the establishment of the magnitude sequences. The Bruce plates were made by Dr. J. S. Paraskevo-

TABLE 1

SUMMARY OF PLATES AND COUNTS

PLATE	RA (1900)	DEC.	λ	β	Q	m_e	m_n	N_{tot}	N_{18}	N_9
A 20280	$22^h48^m.8$	$-10°16'$	27°.1	$-58°.4$	6	18.4	17.7	1265	1031	340
20318	22 49.9	5 17	35.9	55.4	8	18.3	17.9	2208	1867	729
17182	22 59.3	15 20	23.3	63.4	6	18.6	18.3	797	677	295
15781	23 19.2	0 18	51.6	56.2	5	18.0	17.5	603	546	233
17777	23 40.2	15 13	39.6	71.1	5	18.6	18.5	1343	1177	537
20484	23 59.1	17 38	45.6	76.0	8	19.6	18.4	1641	1441	741
20341	23 59.6	5 23	65.2	65.4	8	18.7	18.3	2495	2078	811
19788	0 18.8	10 17	72.1	71.6	5	18.2	18.0	1383	1138	448
20347	0 18.9	0 31	78.7	61.9	7	18.4	18.2	2892	2457	988
17867	0 19.0	15 16	68.0	76.4	7	18.9	18.8	1838	1601	769
20503	0 38.0	20 20	86.5	82.3	5	18.9	18.2	1656	1538	686
17084	0 39.0	0 20	89.5	62.3	6	18.2	17.7	896	664	308
16253	0 40.0	10 06	90.0	72.1	7	18.5	18.1	1528	1247	588
18691	0 58.9	15 18	110.1	76.6	7	19.3	18.8	4510	3847	1341
16213	1 20.0	10 36	120.3	70.2	6	18.4	18.1	906	740	293
18706	1 38.5	15 15	139.6	71.4	5	18.3	17.6	1021	854	391
18809	1 56.3	20 30	160.8	71.1	6	17.9	17.8	664	575	230
15814	1 58.3	0 14	127.3	56.5	5	18.4	18.0	891	781	299
20440	1 59.3	15 16	149.1	67.7	8	18.4	17.8	1781	1547	796
17946	2 19.3	15 12	156.1	63.7	5	18.1	17.8	1962	1711	839
20433	2 19.5	20 17	166.7	66.3	7	18.2	17.9	2265	1997	905
17971	2 38.0	20 19	170.6	62.1	6	18.9	18.6	2128	1839	951
Means and totals					6.2	18.5	18.1	36,673	31,353	13,518

poulos and his assistants at the Boyden Station. Miss Boyd and Miss Martha Dowse have assisted throughout with the calculations and editorial details.

2. The Observational Material.—Twenty-two plates, each of three hours' exposure with the Bruce refractor at Bloemfontein, have been used in the present investigation. Because of the general unreliability of faint magnitude standards south of declination $-23°$, only plates in the northern part of the south galactic cap were used. In this area both the van Rhijn and the Seares and Joyner tables have been employed in setting up the stellar magnitude sequences. Although the magnitude scale is not as cer-

tain as one could wish fainter than magnitude 17.5, it has the security of being based on the Mount Wilson values of the Selected Area sequences in declinations $-15°$ and $0°$.

In table 1 the twenty-two plates are listed in order of right ascension. The fourth and fifth columns contain the galactic longitudes and latitudes, and the sixth the qualities of the plates (10 represents perfection) from the standpoint of satisfactory discovery and measurement of nebulous objects. The seventh and eighth columns give, respectively, the magnitude m_s of the faintest stars easily visible on the plates and the magnitude m_n to which the nebular survey is judged to be complete. The average difference between these two limiting magnitudes, and its mean error, are

$$\overline{m_s - m_n} = 0.42 \pm 0.06.$$

The values are similar to those obtained heretofore in similar studies.

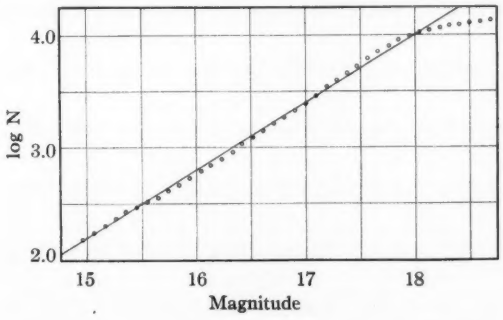

FIGURE 2

Magnitude frequency for all plates. Abscissae are photographic magnitudes corrected for red shift; ordinates are logarithms of the cumulative totals. The straight line is defined by (2).

The last three columns of table 1 give the total number of nebulous objects marked on the plate, the total number in the central twenty-five square degrees, and the total for the central nine square degrees where distance correction can be ignored and there is diminished probability of error of misidentification through deformed images. The grand totals for the whole plate and for the twenty-five square degrees include about twelve hundred and one hundred objects, respectively, that are twice counted through overlapping. Some of these plates appear in an earlier tabulation[3] with totals and magnitude limits differing somewhat from the present values which represent further measurement and analysis.

The magnitudes in intervals of $0^m.1$ are assembled for each plate in table 2. Although the magnitudes of all objects in the central twenty-five square

TABLE 2

THE DISTRIBUTION OF MAGNITUDES FOR TWENTY-TWO PLATES

	]15.0	15.0	15.1	15.2	15.3	15.4	15.5	15.6	15.7	15.8	15.9	16.0	16.1	16.2	16.3	16.4	16.5	16.6	16.7	16.8
A 20280	4	1	0	0	1	1	3	1	2	1	2	4	1	2	4	1	4	2	3	7
20318	4	0	0	0	2	3	3	1	2	4	0	3	3	3	3	7	3	8	12	14
17182	0	0	1	1	0	1	0	0	0	0	1	0	0	1	0	0	1	2	3	4
15781	4	0	0	3	1	5	0	2	1	1	2	2	2	2	1	0	4	5	5	8
17777	1	0	0	1	0	2	0	2	1	0	1	0	2	1	1	2	0	5	3	3
20484	3	0	1	1	2	0	1	1	1	3	2	3	1	4	3	4	8	5	4	4
20341	13	2	2	3	0	2	1	3	1	5	2	4	3	3	4	4	10	4	11	10
19788	6	3	1	0	1	2	0	2	1	1	3	2	3	4	3	4	7	4	4	3
20347	2	1	2	2	1	0	1	3	1	8	4	3	6	5	7	15	23	15	22	25
17867	5	5	1	1	1	3	2	0	2	7	2	3	3	0	8	4	4	4	6	6
20503	10	1	0	0	2	0	3	1	3	2	1	1	0	1	0	3	6	4	7	6
17084	7	0	3	2	3	2	0	1	0	2	2	3	4	10	8	3	6	9	5	9
16253	13	2	2	0	4	0	1	3	3	5	5	3	7	4	6	6	6	18	10	15
18691	2	0	4	2	3	2	1	2	2	1	5	6	14	10	9	16	9	11	4	11
16213	2	0	2	0	3	3	2	0	0	1	2	3	0	2	2	5	2	6	2	9
18706	7	2	2	2	0	1	3	0	1	6	2	8	9	3	12	8	9	6	13	17
18809	1	0	1	0	0	0	0	1	0	0	1	0	0	1	2	5	0	7	3	4
15814	3	0	0	1	1	1	1	0	0	0	1	0	1	4	4	4	6	3	5	6
20440	1	1	0	0	2	1	0	3	3	0	7	3	2	7	7	10	15	8	14	16
17946	4	2	1	0	2	0	0	1	2	2	4	2	9	4	7	9	11	9	10	10
20433	17	5	2	4	2	3	1	2	0	5	2	4	3	9	4	8	11	12	10	20
17971	15	1	2	4	1	2	1	5	2	6	5	5	6	3	4	8	9	9	14	4
22 Plates	124	26	27	27	32	34	24	34	28	60	56	62	79	83	99	126	154	156	170	211
13 "	75	15	18	16	19	18	14	22	17	39	34	33	46	42	51	75	91	90	95	106
5 "	26	6	8	9	7	9	5	10	8	17	15	17	26	18	25	34	30	34	31	28
Log tot 22	2.09	2.18	2.25	2.31	2.37	2.43	2.47	2.52	2.55	2.62	2.67	2.73	2.79	2.84	2.90	2.96	3.03	3.09	3.15	3.21
" " 13	1.88	1.95	2.03	2.09	2.16	2.21	2.24	2.29	2.33	2.40	2.46	2.51	2.56	2.61	2.66	2.73	2.80	2.85	2.91	2.96
" " 5	1.41	1.51	1.60	1.69	1.75	1.81	1.85	1.90	1.94	2.02	2.08	2.14	2.21	2.26	2.31	2.38	2.43	2.48	2.53	2.56

	16.9	17.0	17.1	17.2	17.3	17.4	17.5	17.6	17.7	17.8	17.9	18.0	18.1	18.2	18.3	18.4	18.5	18.6	18.7	[18.7
A 20280	10	19	18	30	21	22	23	30	35	28	25	12	15	6	2					
20318	16	33	19	36	30	27	42	45	74	69	81	66	62	38	16					
17182	4	5	4	8	4	7	12	13	11	20	24	23	21	20	34	29	29	11	1	
15781	6	13	15	30	21	30	27	10	14	6	10	3								
17777	4	14	8	6	17	13	23	18	21	34	43	36	28	47	37	57	66	32	8	
20484	4	11	11	10	20	20	16	20	16	21	26	31	21	44	52	71	74	46	51	125
20341	15	13	10	24	20	29	35	42	46	61	45	35	43	51	63	62	72	43	15	
19788	2	6	7	11	16	21	27	36	42	46	54	61	43	19	3					
20347	19	16	22	27	25	31	48	56	48	60	82	77	103	101	84	38	5			
17867	5	3	8	11	13	10	16	15	18	25	29	31	18	29	28	40	37	60	80	226
20503	9	12	13	14	27	37	33	32	34	44	39	49	35	42	41	40	48	49	32	5
17084	10	10	8	19	19	21	17	21	31	21	21	12	8	9	2					
16253	20	19	23	22	23	26	28	26	30	38	42	49	67	27	19	14	2			
18691	13	11	11	28	21	19	22	35	37	39	30	43	54	66	98	83	101	106	115	295
16213	5	5	4	10	10	8	13	10	21	14	31	31	30	32	16	6	1			
18706	26	15	18	23	26	28	24	32	26	16	17	14	10	2	3					
18809	7	8	13	7	10	17	20	30	22	28	29	13								
15814	1	4	10	11	4	11	9	11	17	42	42	43	32	14	7					
20440	19	15	31	41	51	58	58	69	71	72	65	52	46	28	16	4				
17946	9	10	21	46	45	48	51	63	105	115	106	79	42	10						
20433	16	25	23	21	21	30	39	69	85	94	123	108	79	41	7					
17971	8	11	13	24	38	25	43	34	33	30	51	37	37	49	34	54	79	84	80	81
22 Plates	228	278	310	459	482	538	626	717	837	923	1015	905	794	675	562	498	514	431	382	732
13 "	109	130	144	206	238	257	325	348	374	474	538	546	532	541	516	494	514	431	382	732
5 "	34	50	51	79	109	87	120	122	125	149	179	178	158	235	249	305	357	328	334	727
Log tot 22	3.26	3.33	3.39	3.46	3.53	3.59	3.66	3.72	3.78	3.85	3.90	3.95	3.99	4.02	4.04	4.06	4.08	4.09	4.11	
" " 13	3.01	3.06	3.11	3.18	3.24	3.30	3.37	3.43	3.48	3.55	3.61	3.66	3.71	3.75	3.79	3.83	3.86	3.88	3.90	
" " 5	2.60	2.65	2.70	2.76	2.84	2.89	2.95	3.01	3.06	3.11	3.17	3.22	3.26	3.31	3.36	3.41	3.47	3.52	3.56	

degrees have been measured, only the homogeneous data for the nine central square degrees on each plate are tabulated and used for the present magnitude-frequency discussion. For plate *A* 18691 the nebular counts were made on eight square degrees only, because the ninth contains the rich cluster of galaxies described in these PROCEEDINGS for November, 1939; to correct for the omission, the numbers counted in the eight square degrees have been multiplied by the factor 9/8. At the bottom of the table are totals, sub-totals and logarithms of the cumulative totals and sub-totals, used below in section 3.

The plates are not equally potent; some penetrate to nearly twice the depth of others as indicated by the values of m_s and m_n in table 1.

3. Discussion.—Table 2 shows the usual diversity in the distribution of magnitudes, illustrated in figure 1 by the data from three plates (central nine square degrees). Similar unevenness is sometimes manifest on a single plate.

Plate *A* 20433 is rich, and down to magnitude 17.5 the frequency fits fairly well the theoretical uniform-density curve (1) for $m_1 = 15.2$, which is the average value for the south galactic cap;[4] but apparently a cloud of nebulae is encountered at about magnitude 17.5, doubling the "uniform" number at magnitude 17.8. (A large error in the magnitude scale appearing abruptly at 17.4 would account for the deviation, but is improbable.)

In contrast, plate *A* 20503 is poor, and reaches the "average" curve only at 17.3 to 17.5; it then shows a sub-uniform gradient, the space density falling off sharply with distance until the approaching plate limit disturbs the census at about magnitude 18.5. Plate *A* 20341 is better represented by the lower "uniform" curve, with $m_1 = 15.5$ and a clustering of about 150 galaxies centered around $m = 17.6$ at a distance of $r = 10^{0.2(17.6 + 14.2) - 5} = 23$ megaparsecs, than by the average curve. For all three figures the ordinates are not cumulative totals, but are the numbers for nine square degrees in successive tenth-of-a-magnitude intervals, taken directly from table 2 and not corrected for red shift.

All the data of table 2 are represented by a single logarithmic plot in figure 2. The ordinates are logarithms of the total numbers brighter than the corresponding magnitudes (abscissae). Since m_n is brighter than 17.7 for two of the plates, the plot cannot be taken as a dependable representation of magnitude frequency fainter than that magnitude. Before making this and subsequent graphs, and all the following calculations, the magnitudes of table 2 were corrected for the red shift.

The straight line that best represents the total material from 198 square degrees, as plotted in figure 2, is given by

$$\begin{aligned} \log N_t &= 0.600m - 6.806 \\ &\pm 0.011 \quad \pm 0.017 \end{aligned} \tag{2}$$

where the mean errors are computed from a least squares solution. From (1) we have

$$m_1 = 15.17 \pm 0.03$$

when we reduce the result (2) to one square degree by the relation

$$\log N_i - \log 198 = \log \overline{N} = 0.600\,(m - m_1).$$

Equation (2) would require, for the area covered by the present survey, eight galaxies brighter than 12.9. An examination of the Shapley-Ames catalog for the central nine square degrees of these twenty-two plates shows three systems, as follows:[5]

NGC 175	$12^m.8$
247	10.7
908	11.1

The relatively small population of bright galaxies in the southern galactic hemisphere has been generally recognized.

The investigation of the magnitude-frequency relation can be carried to fainter magnitudes than involved in (2) by including in the totals and graphs only the data from plates with faint magnitude limits. We thus have in figure 3 two graphs referring to 117 and 45 square degrees, and essentially complete for objects as faint as magnitudes 18.2 and 18.6, respectively. The corresponding linear solutions are given by

$$\begin{aligned} \log N_{117} = {} & 0.589m - 6.871 \\ & \pm 0.006 \quad \pm 0.009 \end{aligned} \tag{3}$$

$$\begin{aligned} \log N_{45} = {} & 0.571m - 6.981 \\ & \pm 0.006 \quad \pm 0.012 \end{aligned} \tag{4}$$

which yield the values

$$\begin{aligned} m_1 &= 15.18 \pm 0.015, \\ m_1 &= 15.12 \pm 0.02. \end{aligned}$$

Giving weights 3, 2, 1, respectively, to the three determinations of b and m_1, we obtain the mean results

$$\begin{aligned} \bar{b} &= 0.592 \pm 0.009 \text{ (m. e.)}, \\ \overline{m_1} &= 15.16 \pm 0.02 \text{ (m. e.)}. \end{aligned} \tag{5}$$

Again it is found that there should be eight galaxies brighter than 12.9 in the 198 square degrees.

4. The best representation of the magnitude-frequency plots for individual plates cannot be obtained by linear formulae. The considerable deviations from uniformity in space density, already shown by the plots in

figure 1, and the frequencies in table 2, can be further illustrated by calculating the distribution constants, b and m_1, at various right ascensions. It happens that the plates used in computing both the values (3) and (4) are well distributed in right ascension and thus those computations do not provide a test of variation of density across the galactic cap. Assembling the material into three groups of seven plates each,† we obtain the following values and mean errors for the radial gradient and the space-density parameter:

	I	II	III
b =	0.632	0.571	0.611
	± 0.024	± 0.009	± 0.020
m_1 =	15.43	15.06	15.09
	± 0.05	± 0.02	± 0.05

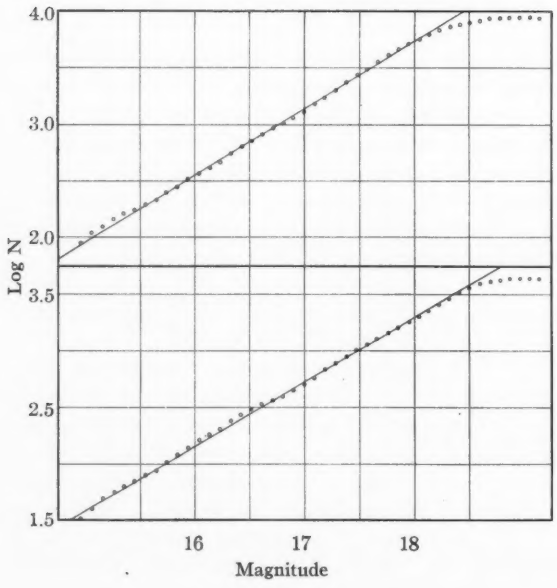

FIGURE 3

Magnitude frequency for thirteen plates (above) and five plates. Coördinates as in figure 2. The straight lines are defined by (3) and (4).

From the measures of m_1 it is seen that the density increases conspicuously with increasing right ascension; a decrease of 0.35 in the parameter corresponds to an increase of about sixty per cent in the space density.

† Plate *A* 18691 is omitted.

In earlier communications[1] attention has been called to the metagalactic gradient that crosses the south galactic cap and extends to the southeastward, nearly to the Milky Way. The plates now under examination lie wholly in the first and second quadrants, but they also show this transverse gradient which appears most conspicuously when first and third quadrants are intercompared.

TABLE 3

RADIAL GRADIENTS AND SPACE DENSITY PARAMETERS

PLATE	b	m_1	PLATE	b	m_1	PLATE	b	m_1
A 20280	0.67	15.48	20347	0.72	15.24	18706	0.63	15.00
20318	0.76	15.41	17867	0.48	14.88	18809	0.87	16.18
17182	0.78	16.37	20503	0.58	15.16	15814	0.60	15.73
15781	0.63	15.44	17084	0.52	14.90	20440	0.86	15.56
17777	0.75	16.01	16253	0.53	14.62	17946	0.75	15.38
20484	0.62	15.50	18691	0.58	14.92	20433	0.52	14.44
20341	0.57	14.88	16213	0.57	15.41	17971	0.49	14.46
19788	0.57	15.23						

The irregularities in space distribution and possibly in luminosity spread are further shown by a graphical determination of the constants for each plate separately. The results are given in table 3, where the plates are listed in order of right ascension. The gradient b varies from 0.48 to 0.87; m_1 is systematically fainter for the first part of the table. The mean values and their mean errors are

$$\bar{b} = 0.64 \pm 0.025,$$
$$\overline{m_1} = 15.28 \pm 0.11.$$

5. *Summary.*—(*a*) The total photographic magnitudes of something more than thirty-one thousand galaxies have been twice estimated on twenty-two Bruce plates, each of three hours' exposure, on fields in the south galactic polar cap.

(*b*) The magnitude system for the nebulae is based on that provided for stars through the international standards in Selected Areas; the sequences have been set up by the star-count method.

(*c*) The high latitude areas covered by this study are free of inequalities in space absorption, if we judge by the distribution of the faint stars; and probably the total dimming of light by interstellar or intergalactic absorption does not here exceed a quarter of a magnitude.

(*d*) In the coefficients b of table 3 and in the frequency curves of figure 1 we have numerical and graphical illustration, for this favorably explored region, of the usual deviations from uniformity in the space distribution of galaxies.

(*e*) In figures 2 and 3 we have what is probably the best information yet

obtained on the magnitude frequency of galaxies in absorption-free non-cluster regions. A good determination of the *average* space-density parameter is therefore possible for this section of intergalactic space. The value $\overline{m}_1 = 15.16 \pm 0.02$ (m. e.) is derived by a least squares discussion of the assemblages of data used for figures 2 and 3, and 15.28 ± 0.11 (m. e.) from the twenty-two individual values graphically determined for table 3.

(*f*) Evidence is again found of the strong transverse metagalactic density gradient, across the south galactic cap; but in the line of sight, when all plates are considered together (13,518 objects), the changes of density with distance scarcely exceed the error of measurement. The adopted mean value of the line-of-sight gradient is $\bar{b} = 0.592 \pm 0.009$ (m. e.).

(*g*) Taking $\bar{b} = 0.6$ (uniform space density), we have in the present result an indication of the necessity of the red-shift correction to the photographic magnitudes; of more importance, we have an intimation of the relatively high accuracy of the stellar and nebular magnitude scales from the fifteenth to the eighteenth magnitudes. A systematic error in the scale as large as five per cent is not possible in the mean curves (figures 2 and 3), unless it chances to be almost exactly balanced by an unrevealed radial density gradient.

[1] These PROCEEDINGS, **24,** 148, 282, 527 (1938).

[2] Shapley, *Harvard Reprint* **68,** 112–115 (1931); these PROCEEDINGS, **21,** 589–591 (1935); **23,** 450, 452 (1937); and *Harv. Ann.*, **105,** No. 8, 146–149 (1937). Seyfert, *Harv. Ann.*, **105,** No. 10 (1937). Shapley and Jones, *Ibid.*, **106,** No. 1, 5 (1938).

[3] *Harv. Circ.* 423 (1937).

[4] These PROCEEDINGS, **24,** 149 (1938).

[5] *Harv. Ann.*, **88,** No. 2 (1932).

---

*STUDIES IN CALCIUM METABOLISM WITH THE AID OF ITS INDUCED RADIOACTIVE ISOTOPE. I**

BY W. WESLEY CAMPBELL AND DAVID M. GREENBERG

DIVISION OF BIOCHEMISTRY, UNIVERSITY OF CALIFORNIA MEDICAL SCHOOL

Communicated February 13, 1940

"Tracer" studies with induced radioactive isotopes have led to important results in the field of mineral metabolism.[1] Calcium is one of the most important of the biological mineral elements. It is one in the study of which a radioactive isotope of calcium as a "tracer" would be very desirable.

The metabolism of calcium is a slow process, and a relatively long time is required for changes to take place. For this reason, the hitherto known radioactive isotope of calcium,[2] with a half life of only about 2.4 hours, has

not been suitable. Furthermore, Walke[3] has shown that this isotope, Ca^{49} (previously believed to be Ca^{45}), disintegrates to form radioactive $Sc.^{49}$ Any studies, then, with Ca^{49} would be complicated and invalidated by the continuously formed radioactive scandium impurity.

Recently, Walke has reported[3] that Ca^{45} is radioactive with a half life of about 180 days. This isotope disintegrates to an inactive scandium with the emission of a very soft β-radiation. The radiation of Ca^{45} is so soft that it cannot be measured satisfactorily in metabolism studies with the electroscope, with the FP-54 electrometer,[4] nor with glass or metal-wall Geiger-Müller counter tubes. Highly successful measurements can be made with the screen-wall G-M tube described by Libby.[5, 6]

This communication is a report of a test study on the suitability of the new radioactive calcium isotope for biological investigations. It was found that, with appropriate care, results of great accuracy can be obtained.

Experimental Methods.—A sample of radioactive calcium was prepared in the Radiation Laboratory† by the bombardment of calcium metal with 8 m. e. v. deutrons in the cyclotron according to the following nuclear reaction:

$$_{20}Ca^{44,48} + {}_{1}H^{2} \longrightarrow {}_{20}Ca^{45,49} + {}_{1}H^{1}.$$

After allowing about six weeks to elapse in order that the Ca^{49} and Sc^{49} might disintegrate to negligible amounts, the metal containing the Ca^{45} was dissolved in a dilute HCl solution. Small amounts of inactive NaCl and HCl were added to serve as carriers for the separation of traces of radioactive Na and K. The calcium was precipitated as the oxalate. The precipitate was dissolved in dilute HCl and reprecipitated as the oxalate a second time. The calcium oxalate was then converted to the calcium carbonate by ignition in an electric muffle. This was dissolved in sufficient lactic acid to form a 5 per cent calcium lactate solution. About 8 ml. were obtained.

Five ml. of this 5 per cent calcium lactate solution were given by stomach tube to a male adult rat, weighing 259 grams, and which had been kept without food for 24 hours. Immediately after the administration of the calcium lactate solution, the animal was placed in a wire metabolism cage over a urine-feces separating device.[7] The feces and urine were collected separately at intervals over a period of about 69 hours. A normal diet was supplied ad libitum to the animal 18 hours following the administration of the calcium lactate.

At the end of about 69 hours, the rat was anesthetized with chloroform and sacrificed by withdrawing blood by cardiac puncture. The blood was allowed to clot and the serum was collected. The viscera were removed and the animal was skinned. The contents of the large intestine were washed out and added to the final fecal collection. The residual carcass,

which weighed 156 grams, was boiled in 1:5 NH_4OH solution, and allowed to stand in the solution for several days to separate the muscles from the skeleton. The teeth were separated from the bones. The various tissues then were dried and dry ashed at 500°C. The ash in each case was dissolved in dilute HCl solution, and the total solution or an appropriate aliquot was used for analysis. The calcium was precipitated as the oxalate according to the standard analytical procedure. The calcium oxalate precipitate was collected on a 4.25 cm. No. 1 Whatman filter paper, and finally washed with an 0.02–0.03 per cent agar solution to prevent mechanical loss of the precipitate when dry.

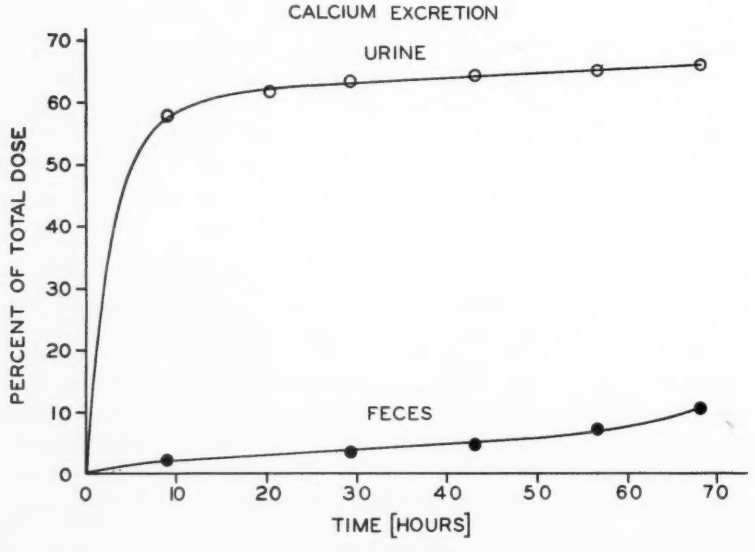

FIGURE 1

Studies in calcium metabolism with the aid of its induced radioactive isotope. I.

The calcium in 0.0976 ml. of the original calcium lactate solution was precipitated and treated in a similar manner to serve as a standard for comparison of activity. All radioactivity measurements were made on the screen-wall counter. The sum of the measured activities of the excreta and of all of the tissues showed a recovery of 103 per cent of the Ca^{45} given, so that all figures have been corrected by the factor 100/103.

Results.—Figure 1 shows graphically the excretion of Ca^{45} during the approximately 69 hours following administration. The amount appearing ing the feces was 10.8 per cent. This means that at least 89.2 per cent was absorbed from the alimentary tract. The apparently increasing rate of

excretion in the feces may indicate an excretion of calcium into the intestines. If this were true, the amount absorbed actually would have been a little greater than 89.2 per cent. Of the 89.2 per cent absorbed, 57.9 per cent appeared in the urine during the first 9 hours after administration. The rate of excretion by way of the urine then dropped off rapidly, a total of 65.6 per cent appearing in the urine. This is in harmony with the work of Greenberg and Gunther[8] who showed that certain calcium compounds, including the lactate, caused a marked increase in the diffusible calcium of the blood, which reached a peak two hours after ingestion, and returned to normal within about 4 hours.

TABLE 1

DISTRIBUTION OF RADIOACTIVE CALCIUM

TISSUES	WEIGHT, GM. FRESH	WEIGHT, GM. DRY	PER CENT TOTAL DOSE CONTENTS IN WHOLE TISSUE	PER CENT TOTAL DOSE CONTENTS PER GRAM FRESH WT.	PER CENT TOTAL DOSE CONTENTS PER GRAM DRY WT.
Bones		8.94	19.9 ± 1.76		2.23 ± 0.20
Teeth		0.410	1.13 ± 0.25		2.75 ± 0.61
Blood Serum	5.095	0.358		0.007 ± 0.001	0.094 ± 0.009
Muscle		45.08	0.76 ± 0.066		0.017 ± 0.001
Skin and Hair	51.19	23.88	1.43 ± 0.15	0.028 ± 0.003	0.060 ± 0.006
Stomach	1.86	0.544	0.008 ± 0.004	0.004 ± 0.002	0.015 ± 0.008
Small Intestine	5.87	1.65	0.099 ± 0.008	0.017 ± 0.0014	0.060 ± 0.005
Large Intestine	1.66	0.62	0.037 ± 0.006	0.022 ± 0.004	0.060 ± 0.010
Liver	9.62	3.06	0.049 ± 0.005	0.005 ± 0.0001	0.017 ± 0.002
Kidney	2.07	0.53	0.007 ± 0.001	0.003 ± 0.0004	0.013 ± 0.002
Spleen	0.79	0.19	0.008 ± 0.003	0.010 ± 0.0037	0.042 ± 0.015
Heart	0.84	0.19	0.017 ± 0.004	0.020 ± 0.0047	0.089 ± 0.021
Lung	0.45	0.27	0.018 ± 0.006	0.040 ± 0.013	0.067 ± 0.022
Testes	5.48	2.71	0.031 ± 0.006	0.006 ± 0.0012	0.012 ± 0.002

The unexcreted Ca^{45}, which amounted to 23.6 per cent, was found to be distributed as shown in table 1. As expected, the largest amount of the retained calcium was found in the bones. However, significant amounts were found in the skin and in the teeth. Because of its large mass, the total accumulation of Ca^{45} in the skin is considerable, but the specific retention is not so great as in some other tissues. In the case of the teeth, the specific retention of Ca^{45} is at least as great as, if not greater than, that in the bones. This would indicate that the calcium of certain parts of the teeth is as mobile as that of the bones.

The concentration of Ca^{45} remaining in the serum is small. The specific retention in the small intestine, large intestine, heart and lung is about the same as that in the skin, and is extremely low in the other tissues examined. The small amounts present perhaps are significant, but could be accounted for, at least in part, by occluded blood.

Summary.—1. Radioactive Ca^{45}, with a half life of 180 days, is suitable for use in "tracer" studies if the radioactivity is measured with a screen-wall counter tube.

2. The radioactivity measurements of a sample of Ca^{45}, administered to a rat, showed quantitative recovery in the summation of the measurements on excreta, bone, tooth, skin, carcass, blood and viscera.

3. In a post absorptive state, the rat absorbed at least 89.2 per cent of the calcium given by stomach tube, and excreted 65.6 per cent in the urine.

4. The specific retention of calcium fell off in the following order: highest in bone and teeth, which were about equal; intermediate in small intestine, large intestine, heart, lung and skin; and least in there maining tissues.

We are indebted to Professor E. O. Lawrence, Dr. Harold Walke and the staff of the Radiation Laboratory of the University of California for the radioactive calcium used in this experiment. Our thanks are due also to Professor W. F. Libby for making many of the radioactivity measurements for us with the screen-wall counter, and for allowing us the use of the counter to make the remainder of the measurements.

* Aided by a grant from the John and Mary R. Markle Foundation. Technical assistance was furnished by the personnel of WPA Official Project No. 65-1-08-62.

† Kindly prepared by Dr. H. Walke, whose recent untimely death lamentably cut short a brilliant scientific career.

[1] Lawrence, J. H., *Handbook of Physical Therapy*, Am. Med. Assoc., 1938; Hevesy, G., *Enzymologia*, **5**, 138 (1938), *Jour. Chem. Soc.*, 1213 (1939); Greenberg, D. M., *Ann. Rev. Biochem.*, **8**, 269 (1939).

[2] Walke, H., *Phys. Rev.*, **51**, 439 (1937).

[3] Walke, H., *Phys. Rev.*, **57**, 177 (1940).

[4] Du Bridge, L. A., and Brown, H., *Rev. Sci. Inst.*, **4**, 532 (1933).

[5] Libby, W. F., *Phys. Rev.*, **46**, 196 (1934).

[6] Libby, W. F., and Lee, D. D., *Ibid.*, **55**, 245 (1939).

[7] Gross, L., and Connell, S. V. B., *Jour. Physiol.*, **57**, p. 1x (1923).

[8] Greenberg, D. M., and Gunther, L., *Arch. Int. Med.*, **50**, 855 (1932).

SOME BIOLOGICAL EFFECTS OF NUCLEAR DISINTEGRATION PRODUCTS ON NEOPLASTIC TISSUE*

BY P. GERALD KRUGER[1]

CROCKER LABORATORY, UNIVERSITY OF CALIFORNIA, BERKELEY, CALIFORNIA

Communicated February 6, 1940

Experiments of the type described below were initiated in the autumn of 1938 by Professors B. V. Hall, M. Goldhaber and the author at the Physics Department of the University of Illinois. Since the neutron intensity from the small cyclotron there was insufficient to give any conclusive result, the experiments have been continued in the Crocker Radiation Laboratory where intense neutron sources are available.

In the past, neoplastic tissue has been irradiated with x-ray, γ-rays and fast neutrons. In the case of x-ray and γ-ray irradiation the destructive ionization in the tissue is produced by Compton electrons, photoelectrons or positive-negative pair electrons which are ejected or created by the x-rays and γ-rays. The physical processes involved here are well known, and the resulting ionization per unit distance along the path of the electron is small as compared to heavy particle ionization.[2]

The process of neutron irradiation is quite different from the above, since it involves a collision process between two heavy particles instead of between a photon and an electron. Here the recoil proton obtains energy (varying from zero to the neutron energy) from the neutron and dissipates the energy by producing along its path an ionization which is much more intense than that produced by electrons.[2]

In the experiments discussed below, the ionizing bodies are the disintegration products produced when boron is bombarded with slow neutrons. In nuclear terms the reaction is represented by ${}_5B^{10} + n_s^1 \rightarrow {}_3Li^7 + {}_2He^4$. This reaction is one of the most favorable ones known for use in biological experiments of the type here discussed because the capture cross-section for slow neutrons (n_s^1) by boron is about 100 times larger than the collision cross-section for fast neutrons and hydrogen. Thus one would expect this nuclear disintegration process to be more efficient in biology than fast neutron irradiation. Moreover, while the incident slow neutrons have a very small energy (a fraction of an electron volt up to a few electron volts), the disintegration products of the boron slow neutron reaction (${}_3Li^7$ and ${}_2He^4$) have approximately 0.8 m. e. v. and 1.4 m. e. v. energy.[3] These rather large nuclear energies are dissipated in very short distances (approximately 4 and 7 microns) in tissue and so cause an even more intense ionization along their paths than the recoil proton in the fast neutron irradiation process. Thus, from the knowledge of nuclear physics alone, it is clear that the boron slow neutron reaction should cause cell destruc-

tion more efficiently than other types of irradiation, if the disintegration can be produced in the environment of neoplastic cells.

This method has the further potential advantage of localizing the lethal ionization in the region where the boron disintegration takes place and thus removes (in the case of its application to *in vivo* work) the danger of

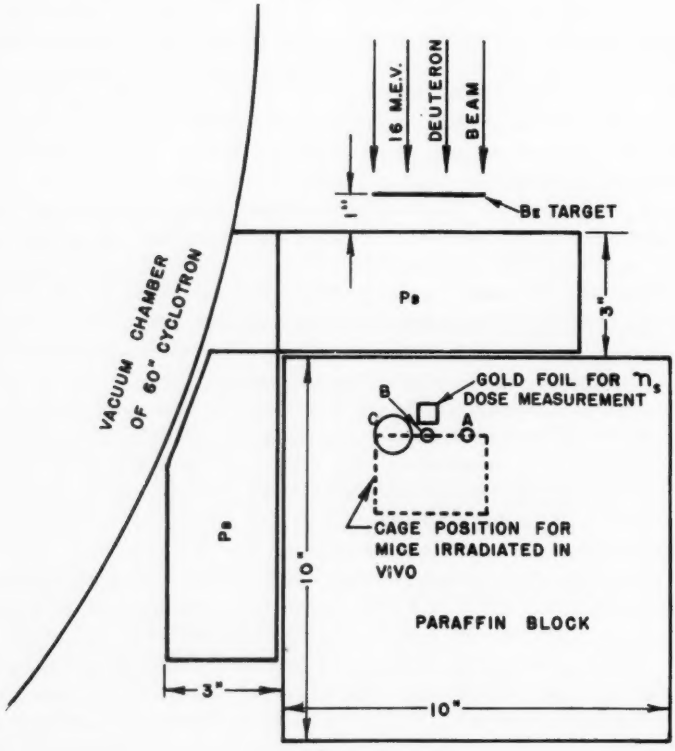

FIGURE 1

Schematic arrangement of beam, target and irradiation positions in the paraffin block.

skin burns and similar disturbing factors which are prevalent in x-ray, γ-ray and fast neutron therapy. This follows from the fact that slow neutrons have so little energy that any ionization caused by a recoil proton from them is negligible. Also it should be remarked that no element having an appreciable concentration in tissue, has a cross-section for slow neutron capture comparable to boron, and thus no ill effects due to slow

neutron irradiation can occur elsewhere in the body. Consequently one can irradiate with large slow neutron doses, provided care is taken to keep the background dose of fast neutrons and γ-rays below the lethal amount.

Figure 1 shows, schematically, the experimental arrangement for producing the slow neutrons used for the irradiations and the relative positions of the irradiated samples in the paraffin block. Fast neutrons are produced, by bombarding Be with 16 m. e. v. deuterons in the 60-inch cyclotron,[4] according to the reaction ${}_4Be^9 + {}_1D^2 \rightarrow {}_5B^{10} + {}_0n^1$. These fast neutrons are slowed down by many collisions with hydrogen nuclei in the paraffin block and are thus available at positions *A*, *B* and *C* for irradiating samples placed at *A*, *B* or *C*. The Pb blocks shown in figure 1 were placed between the target, cyclotron and the irradiated samples to reduce the γ-ray background from the Be target. A thin sheet of gold (Au detector in figure 1) was positioned just in front of hole *B* in the paraffin block and the slow neutron induced radioactivity in the gold used as a measurement of the slow neutron dose for the various irradiations. Measurements of the gold activity were made in the conventional manner using an ionization chamber, amplifier and a scale of four counter. The fast neutron-γ-ray background was measured with a victoreen dosemeter.

The procedure for preparing small pieces of mammary carcinoma, lymphoma and an undifferentiated sarcoma for irradiation and implantation is as follows. A tumor, about ten days old, is taken from the animal and chopped into small pieces suitable for implantation with a trocar. These are placed in a soft glass test tube about $^1/_4$ inch in diameter and immersed in a solution made by adding 2 gm. H_3BO_3 to 100 cc. of buffer solution. Three such samples are made up. One is kept in the laboratory as a control and is not irradiated. This hereafter will be designated as the boron control. A second, the boron irradiated, is placed in position *A* in the paraffin block. The third is placed inside of a one-inch diameter glass tube and the intervening space filled with B_6C. This is placed in position *C* and is designated as a $B + B$ shield. A fourth sample has been prepared for some experiments (mammary carcinoma *A*, *B*, *E* and lymphoma *C*) by omitting the H_3BO_3 from the immersing solution. This is placed in hole *B* and is called the buffer control. All tumors used were known by previous experimentation to give essentially 100 per cent takes for normal implants.

During the course of an irradiation the boron irradiated sample (*A*) receives γ-rays (γ) and fast neutrons (n_f) as background radiation and slow neutrons (n_s). Sample *C* receives mostly background $n_f + \gamma$ radiation, the B_6C absorbing a large part of the slow neutrons except for heavy doses. Thus the resultant differential growth between samples *A* and *C* represents, in a rough way, the effect of the slow neutrons. Sample *B* receives $n_f + \gamma + n_s$ and is simply a control to test for any possible effect

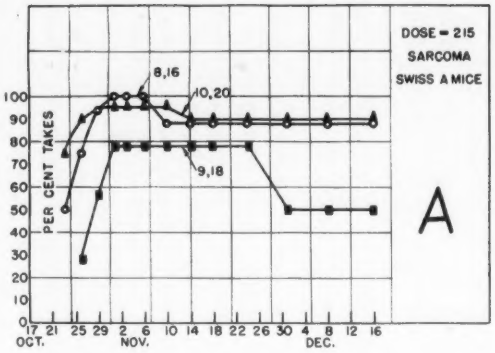

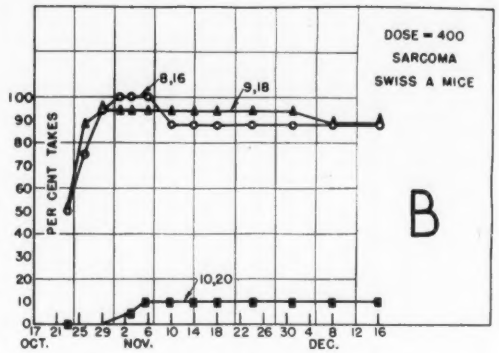

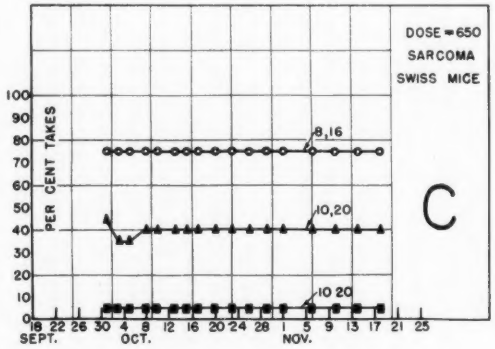

○ B CONTROLS
▲ B + B SHIELD IRRADIATED
■ B IRRADIATED

FIGURE 2

Survival curves for an undifferentiated sarcoma irradiated, *in vitro*, with the disintegration products from the reaction ${}_5B^{10} + n_0{}^1 \rightarrow {}_3Li^7 + {}_2He^4$. Per cent takes are plotted against the number of days after implantation. The first date on the x-axis gives the time of irradiation and implantation.

of irradiation in buffer solution. None was observed as would be expected since none of the elements in the buffer solution have a slow neutron capture cross-section comparable with boron.

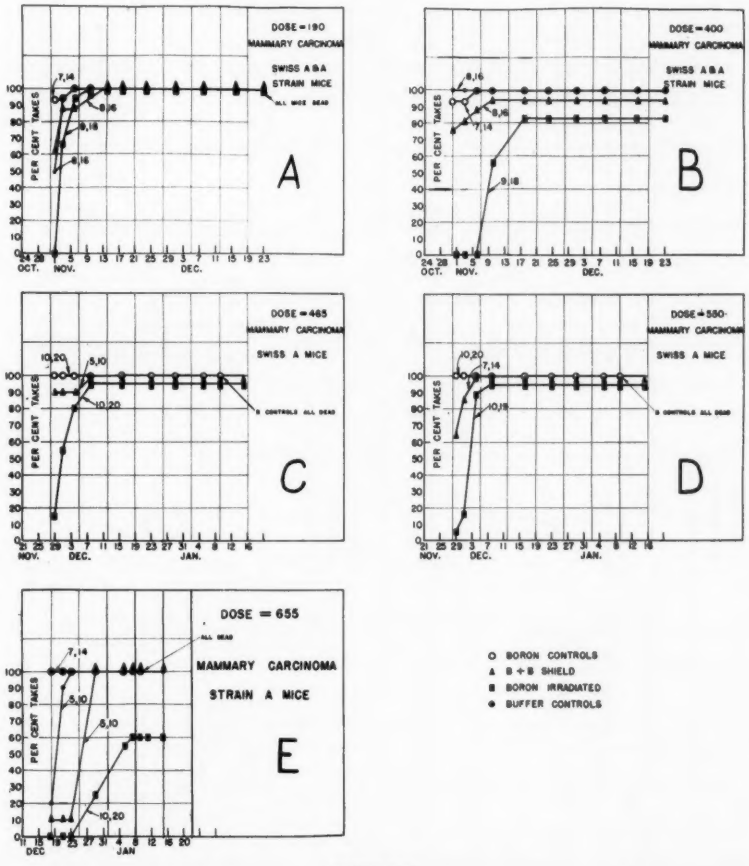

FIGURE 3

Survival curves for mammary carcinoma irradiated, *in vitro*, with the disintegration products from the reaction $_5B^{10} + n_0^1 \rightarrow {}_3Li^7 + {}_2He^4$. Per cent takes are plotted against the number of days after implantation.

After irradiation, two tumor particles are implanted in each mouse (one on each side) used. Thereafter for about eight weeks, the number of takes, for each experiment, was checked at least once a week by counting the number of tumors observable in each mouse and by measuring the

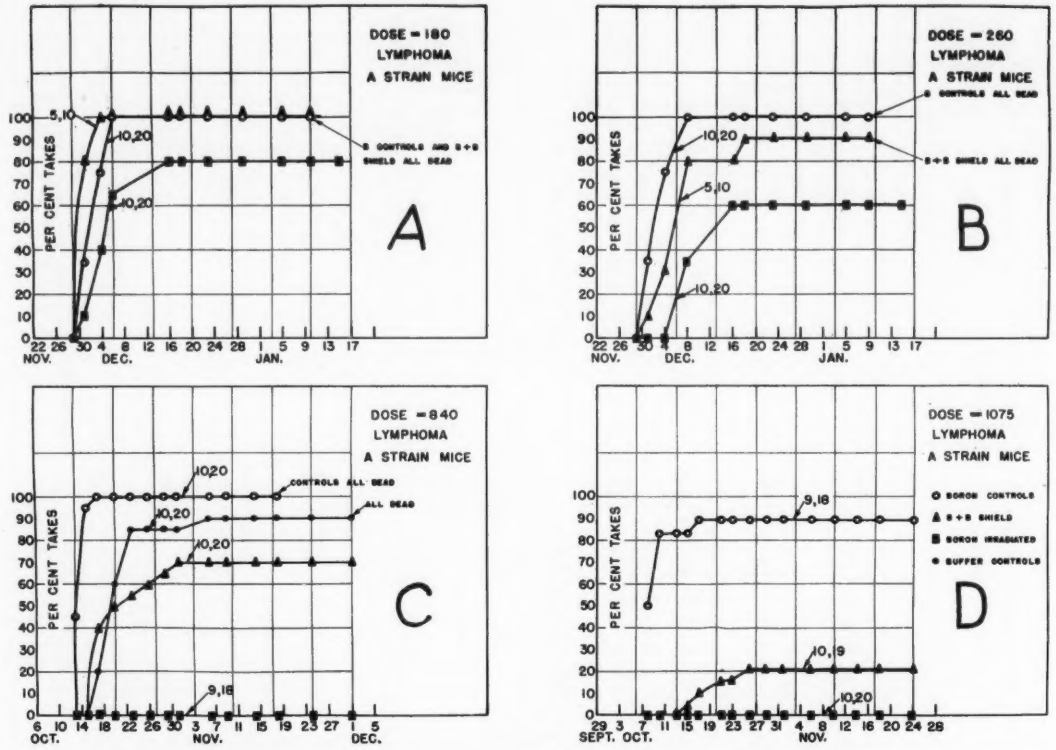

FIGURE 4

Survival curves for lymphoma. Other conditions the same as those of figures 2 and 3.

size of the tumors. The results of these measurements are shown graphically in figures 2, 3 and 4.

Figure 2 shows the effect of the boron disintegration products on an undifferentiated sarcoma which occurred spontaneously in a swiss mouse four years ago, and since then has been observed and studied by Professor B. V. Hall of the University of Illinois. The figure has three sets of curves (*A*, *B* and *C*), one for each of three doses given the tumor particles prepared and irradiated as described above. The dose, given in the upper

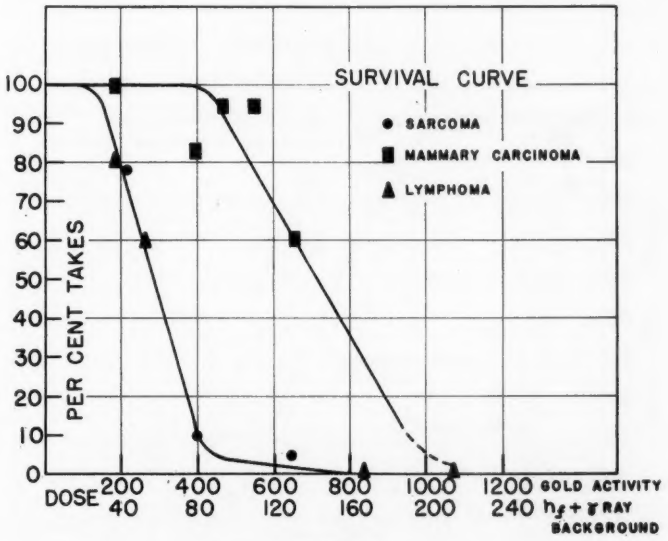

FIGURE 5

Comparison survival curves for sarcoma, mammary carcinoma and lymphoma. Here the maximum per cent number of takes are plotted against the slow neutron dose as measured by gold activity and for reference on another scale the associated $n_f + \gamma$ background dose.

right-hand corner of parts *A*, *B* and *C* of the figure, is the result of the measurement of the radioactivity induced in the gold foil (see Fig. 1) by slow neutrons during the tumor irradiation. For this reason it is a relative dose measurement and, while comparable for all of the experiments described here, has no direct comparison with other dose measurements (i.e., fast neutron doses as measured by a victoreen dosemeter) or even other gold activity dose measurements made under different experimental conditions. Associated with each curve are two numbers, the first one of which gives the number of mice used, the second the number of tumors

implanted (i.e., curve in figure 2*A* for boron irradiated samples has the numbers 9, 18: this means 9 mice and 18 implants).

In a qualitative way the boron shield acts as would be expected. For doses 215, 400 and 650 (Fig. 2*A*, *B*, *C*) the per cent takes are 95, 94 and 40 per cent, respectively. This indicates that for the first two doses enough slow neutrons were absorbed by the B_6C shield so that the transmitted neutrons had little effect on the tumors. However, at dose 650 enough slow neutrons were transmitted to cause 60 per cent deaths. For the

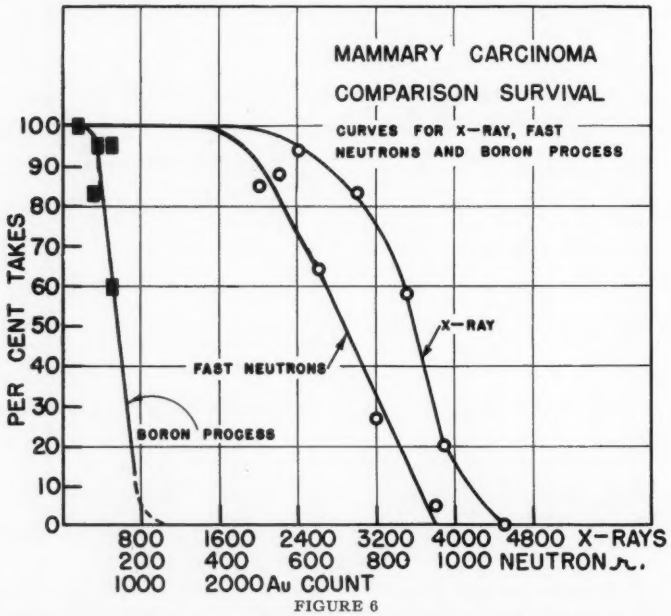

FIGURE 6

Comparison survival curves for mammary carcinoma irradiated with x-ray, fast neutrons and boron disintegration products.

above doses the $n_f + \gamma$ background was approximately 45, 80 and 130 "n." No data concerning the effect of fast neutrons on this sarcoma are available.

Figure 3 shows the effect of the boron disintegration products on mammary carcinoma.[5] The notation here is the same as that for figure 2. In three (*A*, *B* and *E*) of the five experiments performed on this tumor a group of animals were inoculated with implants irradiated in buffer solution as described above. All three groups show 100 per cent takes as was expected from theoretical considerations. The only other similar experi-

ment performed was in part *C* of the lymphoma experiments where 90 per cent takes were observed.

Figure 4 shows the effect of the boron disintegration products on lymphoma.[6] The notation is the same as for figure 2. Here the effect of the boron shield is nicely portrayed. For the doses 180, 260, 840, 1075, the per cent takes for the boron shield irradiated implants are 100, 90, 70 and 21 per cent. The $n_f + \gamma$ background corresponding to the above doses is 35, 50, 170 and 215 "n."

The data in figures 2, 3 and 4 are given in tabular form in table 1.

TABLE 1

SUMMARY OF DATA ON THE *in vitro* IRRADIATION OF SARCOMA, MAMMARY CARCINOMA AND LYMPHOMA WITH DISINTEGRATION PRODUCTS FROM THE REACTION $_5B^{10} + n_0^1 \rightarrow {}_3Li^7 + {}_2He^4$

DOSE FROM GOLD ACTIVITY	APPROXIMATE BACKGROUND $n_f + \gamma$	PER CENT TAKES BORON IRRADIATED	PER CENT TAKES B + B SHIELD	PER CENT TAKES BORON CONTROLS	PER CENT TAKES BUFFER CONTROLS
		Sarcoma			
215	45	78	95	100	
400	80	10	94	100	
650	130	5	40	75	
		Mammary Carcinoma			
190	40	100	100	100	100
400	80	83	94	100	100
465	90	95	100	100	
550	110	95	100	100	
655	130	60	100	100	100
		Lymphoma			
180	35	80	100	100	
260	50	60	90	100	
840	170	0	70	100	90
1075	215	0	21	89	

In figure 5 there is plotted the maximum per cent number of takes (*B* irradiated sample) taken from the curves in figures 2, 3 and 4, vs. the dose for the three tumors used. Here it appears that the sarcoma and lymphoma have about the same sensitivity to the radiation used and that a dose of 450 (gold activity) will kill both kinds of tumors *in vitro*. This corresponds to a $n_f + \gamma$ background of about 90 "n." The mammary carcinoma is more resistant to radiation and needs a dose of about 1000 (gold count) with a background of 200 "n" for 100 per cent lethal effects.

Figure 6 shows a comparison between the effects of x-rays, fast neutrons and boron disintegration products on mammary carcinoma. The x-ray and fast neutron data are taken from curves published by J. H. Lawrence, P. C. Aebersold and E. O. Lawrence.[2]

The fast neutron curve shows that below approximately 500 "n," no failure of takes occurs. Since, for the boron process, the n_f background accompanying the lethal dose (gold activity 1000) of boron disintegration products is only 200 "n," that background cannot be responsible for the lethal effects observed, and one must conclude that the boron disintegration products are responsible for the death of the tumor cells. Another

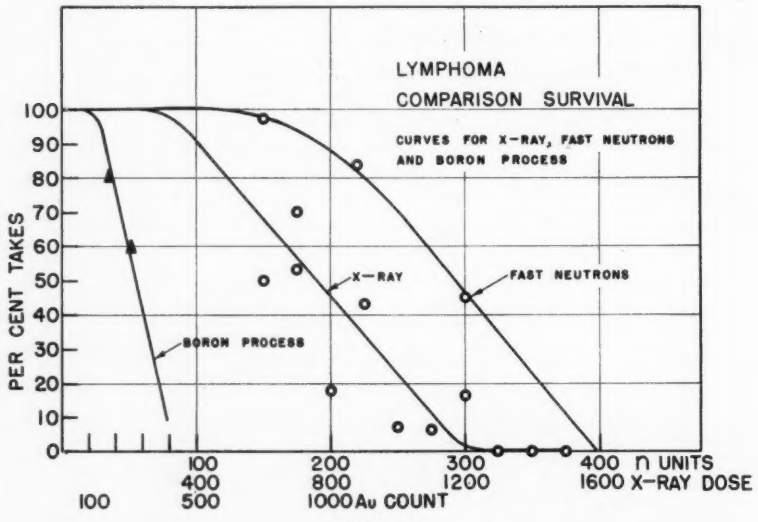

FIGURE 7

Comparison survival curves for lymphoma irradiated with x-rays, fast neutrons and boron disintegration products.

interesting comparison is to note that the dose of fast neutrons for 100 per cent lethal effects is approximately 950 "n," which is about five times the n_f background in the boron process for the same effect. It must be emphasized, however, that the factor five depends on the amount of boron which can be gotten into the tumor and that the factor is meaningless except for the fact that it shows that a sufficient amount of boron can be dispersed throughout the tissue, to accomplish the desired lethal effect.

Figure 7 draws a similar comparison for lymphoma. Here the fast neutron data are taken from preliminary experiments being conducted[7] in the Crocker Radiation Laboratory at the present time and the x-ray

data from exploratory and unconfirmed results. The fast neutron sublethal dose is approximately 175 "n" whereas the $n_f + \gamma$ background accompanying 100 per cent lethal effect in the boron process is about 90 "n" so that again the lethal effects observed here must be due to the boron disintegration products. The fast neutron dose for 100 per cent lethal effect is approximately 400 which is about four times the $n_f + \gamma$ background in the boron process for the same effect.

As shown by the data in table 1, the average per cent number of takes for the boron controls in the three experiments on sarcoma is 92 per cent; for the five experiments on mammary carcinoma it is 100 per cent; and for the four experiments on lymphoma it is 97 per cent. This shows that the boric acid solution when not irradiated has no effect on the growth of these neoplastic tissues.

In considering the data from these experiments, it must be remembered that the number of mice used (see figures 2, 3 and 4) was small so that the shape of the survival curves in figure 5 is known only approximately. It would be of interest to repeat these experiments with a large number of mice to establish the curves more accurately.

In figure 2*A* and *B* there is evidence for some natural regression of the undifferentiated sarcoma. In those cases where regression occurred the tumors grew to good size (1 cc. to 2 cc. volume approximately), became neucrotic and then sloughed off. Eventually some healed completely so that it is unsafe to use this tumor for *in vivo* work.

The results of these *in vitro* experiments also indicate that neoplastic cells can be destroyed *in vivo*, if sufficient boron, in some suitable form, can be applied to the tumor *in vivo*.

Acknowledgment for financial assistance is made to the Dazian Foundation for Medical Research.

It is a pleasure for the author to express his thanks to Professor E. O. Lawrence for the opportunity of working in the Crocker Radiation Laboratory, and to Dr. J. H. Lawrence for his many helpful suggestions and interest in the work.

He also wishes to thank Miss D. Axelrod and Miss V. Condit for their help in preparing and making the tumor implants.

*Acknowledgment is made for assistance from WPA Project No. 10695.

[1] On sabbatical leave from the Physics Department, University of Illinois, Urbana, Illinois.

[2] J. H. Lawrence, P. C. Aebersold and E. O. Lawrence, Occasional Publications, Am. Assoc. Adv. Sci. No. 4, 215–219 (June, 1937).

[3] Bower, Bretcher and Gilbert, *Proc. Camb. Phil. Soc.*, **34**, 290 (1938).

[4] Lawrence, Alvarez, Brobeck, Cooksey, Corson, McMillan, Salisbury and Thornton, *Phys. Rev.*, **56**, 124 (1939).

[5] W. U. Gardner, G. M. Smith, E. Allen and L. C. Strong, *Arch. Path.*, **21**, 265

(1936); J. H. Lawrence, Robert Horn and L. C. Strong, *Yale Jour. Biol. and Med.*, **10**, 145 (1937).

[6] J. W. Lawrence and W. U. Gardner, *Amer. Jour. Cancer*, **33**, No. 1, 112 (May, 1938).

[7] The experiments are being conducted by J. H. Lawrence, P. C. Aebersold and D. Axelrod.

A DECOMPOSITION OF COMPACT CONTINUA AND RELATED THEOREMS ON FIXED SETS UNDER CONTINUOUS TRANSFORMATIONS[1]

BY J. L. KELLEY

DEPARTMENT OF MATHEMATICS, UNIVERSITY OF VIRGINIA

Communicated January 30, 1940

1. Definitions and Theorems on F-sets.—We suppose throughout that M is a compact metric continuum.

DEFINITIONS:[2] A point $p \epsilon M$ is *conjugate* to $q \epsilon M$ provided no point separates p and q in M. If p is a non-cut point, Mp is defined to be the set of all points conjugate to p. $p \epsilon M$ is an *end-point* of M provided there exists an arbitrarily small neighborhood of p having as its boundary a single point. A set is said to be an *F-set* provided it is (1) an end-point of M, (2) a cut point of M or (3) a non-degenerate Mp.

THEOREM 1.1: *Any set Mp may be written as a monotone product $Mp = \pi_1^\infty C_i$, where each C_i is a continuum, the closure of the complement of which consists of a finite number of continua, each intersecting C_i in a single point.*

This theorem is proved by a direct construction, making use of the lemma to the effect that there exists a countable basis for the cut points of M, i.e., a countable set of points $[p_i]$ such that if any two points of M are not conjugate, some point of $[p_i]$ separates them in M. This fundamental theorem implies

THEOREM 1.2: *An F-set is a continuum: the product of an F-set and a continuum is a continuum or vacuous.*

THEOREM 1.3: *M is the sum of its F-sets.*

This theorem is proved by showing that if $p \epsilon M$ is not an end-point and has no conjugate point, it is a cut point. This gives an independent proof of the known result when M is locally connected. For non-locally connected continua the result is new. From this theorem we obtain

THEOREM 1.4: *Each non-cut point of M belongs to one and only one F-set.*

THEOREM 1.5: *In order that two points p and q belong to the same F-set it is necessary and sufficient that p and q be conjugate.*

If p and q are conjugate we obtain a non-cut point conjugate to both, and from this an F-set, by use of the known result that there exists no uncountable collection of mutually conjugate cut points.

As a consequence of 1.1 and the preceding we get

THEOREM 1.6: *If a point p does not belong to a true F-set (i.e., an F-set containing more than one point), it is a regular point in the sense of Menger-Urysohn.*[3]

Also from 1.5 we obtain

THEOREM 1.7: *The product of two F-sets is either a cut point or vacuous. Also, there are in M only a countable number of cut points belonging to true F-sets.*

The proof of the second of these statements requires also the cut point order theorem.[4]

THEOREM 1.8: *In order that a non-degenerate subset of M be a true F-set it is necessary and sufficient that it be separated in M by no point of M, and that it be saturated in M relative to this property.*

This theorem is established on the basis of 1.5.

2. J-sets: F-set reducible and extensible properties.

DEFINITION: A subcontinuum of M is a *J-set* if it is the sum of F-sets.

This is the precise analogue of the A-sets in the cyclic element theory for locally connected continua. We show from 1.2 and 1.5

THEOREM 2.1: *The product of any continuum D with a J-set J is connected.*

From 2.1, we obtain

THEOREM 2.2: *The product of any number of J-sets is either a J-set or vacuous. A J-set J contains all the irreducible continua about any two of its points.*

Analogous to cyclicly extensible and reducible properties we make the following

DEFINITION: A property is *F-set reducible* provided that when M has the property, so also has every F-set in M. A property is *F-set extensible* provided that when every F-set in M has the property, so also has M.

THEOREM 2.3: *Unicoherence is F-set extensible (but not in general F-set reducible).*

If M is locally connected it is known that unicoherence is both cyclicly extensible and reducible.

An example is given showing that the fixed point property is not in general F-set reducible, and that an F-set is not necessarily a retract of the space M.

3. Transformations of a compact continuum into itself.

THEOREM 3.1: *If $T(M) \subset M$ is a continuous transformation of a compact continuum M there exists a continuum $\pi \subset M$, which is a subset of some F-set of M, such that $T(\pi) \supset \pi$.*

Given $T(M)$, it is shown that there exists a continuum N, irreducible

with respect to the property of being the product of continua of type P, where a continuum C is said to be of type P provided the closure of the complement of C consists of a finite number of components D_i, each D_i intersecting C in a single point p_i, and where $T(p_i) \bar{\epsilon} (D_i - p_i)$. It is then shown that N is a subset of an F-set, and finally that N contains a continuum π such that $T(\pi) \supset \pi$.

As results of 3.1 we obtain

THEOREM 3.2: *If $T(M) \subset M$ is a continuous transformation of a compact continuum M, there exists either a fixed point in M or an F-set F such that $F \cdot T(F)$ contains a non-degenerate continuum.*

THEOREM 3.3: *If $T(M) \subset M$ is a continuous transformation of a compact continuum M, there exists a compact subset R of an F-set F of M such that $T(R) = R$.*

THEOREM 3.4: *If $T(M) \subset M$ is a continuous transformation of a compact continuum M which carries each F-set into a subset of an F-set—if, for example, the inverse of no point separates an F-set in M,—then there exists an F-set F such that $T(F) \subset F$.*

In case every F-set is degenerate, we have from 3.4 the Scherrer fixed point theorem for dendrites.[6] If T is a homeomorphism and M is locally connected, 3.4 is Ayres' theorem.[7]

[1] Presented to the Amer. Math. Soc., Dec., 1938. The paper in full was offered to *Fundamenta Mathematicae* for publication in June, 1939.

[2] Compare with Kuratowski and Whyburn, *Fund. Math.*, **16**, 305–331 (1930), and Moore, R. L., *Foundations of Point Set Theory*, p. 72.

[3] $p \epsilon M$ is regular if there exists an arbitrarily small neighborhood of p with a finite boundary. See Menger, *Kurventheorie*, p. 96.

[4] Whyburn, G. T., *Trans. Amer. Math. Soc.*, **30**, 597–609 (1925).

[5] A set $N \subset M$ is a retract of M if there exists a continuous transformation $T(M) = N$ such that T is the identity transformation on N. See Borsuk, K., *Fund. Math.*, **17**, 155 (1931).

[6] *Math. Zeit.*, **25**, 129 (1926).

[7] *Fund. Math.*, **16**, 333–336 (1930).

MINIMAL SURFACES SPANNING CLOSED MANIFOLDS

BY R. COURANT AND N. DAVIDS

NEW YORK UNIVERSITY

Communicated January 26, 1940

The great variety of phenomena presented by the Plateau-Douglas problem is surpassed by the possibilities in the corresponding problems with "free boundaries." In a previous note[1] a simply connected minimal surface of least area was constructed whose boundary consisted partly of a

given Jordan arc and partly of a point-set free on a given manifold, M. In a more detailed paper[2] a doubly connected minimal surface of least area is constructed one of whose boundaries is a prescribed Jordan curve, the other free on a given manifold. The solution of these variational problems is based on a general convergence theorem concerning boundary values of harmonic vectors. (See I or II.)

The present note is concerned with minimal surfaces no part of whose boundary is required to be a monotonically described Jordan curve. Here, as already pointed out in II, an entirely new element enters into the problem and into the existence proof: namely, it becomes necessary to specify the topological position of the required solution relative to the prescribed boundary manifold. This is done by considering linking numbers between the boundary components of the surfaces under consideration and preassigned cycles in the space complementary to the given manifold. Naturally, this viewpoint pertains in a general way to the theory of the Calculus of Variations in the Large for several independent variables and is by no means restricted to the problem of minimal surfaces alone.

In the present note we shall solve the following typical problem for the three-dimensional euclidean space with the position vector $\mathfrak{x}$: given a closed surface M of genus $p > 0$, e.g., a torus; given, furthermore, a closed simple polygon H which has no points in common with M and which is linked with M, i.e., which is linked[3] with all individuals of a class of equivalent non-bounding cycles on M. We seek a simple connected minimal surface of least area whose boundary lies on M [4] and is linked with H, in a sense made precise immediately below. Without a topological condition such as this one the problem would become meaningless, since its solution would then be the degenerate surface $\mathfrak{x} = \text{const}$. According to the choice of H we can, for instance, characterize surfaces filling out the hole in a torus, or spanning the inside of the torus.

Accordingly, we suppose our admissible surfaces to be represented parametrically by $\mathfrak{x}(u, v)$ or $\mathfrak{x}(r, \theta)$ in the unit circle B of the u, v-plane with polar coördinates r, θ. Since the boundary of $\mathfrak{x}$ need not be a continuous curve on M we impose our linking condition in the following manner: we require that all images under $\mathfrak{x}(u, v)$ of simple closed curves in B sufficiently near to the circumference C of B shall be curves arbitrarily near to M and linked with H. Furthermore, we suppose that the first derivatives $\mathfrak{x}_u$ and $\mathfrak{x}_v$ are piecewise continuous in B and that the Dirichlet integral

$$D[\mathfrak{x}] = D_B[\mathfrak{x}] = \tfrac{1}{2}\int\int_B (\mathfrak{x}_u^2 + \mathfrak{x}_v^2)dudv$$

$$= \tfrac{1}{2}\int_0^{2\pi}\int_0^1 \left(\mathfrak{x}_r^2 + \frac{1}{r^2}\mathfrak{x}_\theta^2\right) r dr d\theta$$

exists. We then establish the variational problem: to find an admissible vector $\mathfrak{x}$ for which

$$D[\mathfrak{x}] = d$$

is the smallest possible value. That a solution of this problem yields a minimal surface follows exactly as in the case of the Plateau problem, either with or without the use of conformal mapping. It is the existence proof which requires an essentially new reasoning.

I. Existence Proof.—Denoting by d the greatest lower bound of $D[\mathfrak{x}]$ for admissible vectors we define an "*admissible sequence*" $\mathfrak{x}_n$ as a sequence all of whose members satisfy the admissibility conditions except that the boundary of the surface $\mathfrak{x}_n$ need not be on M, but only on a manifold M_n which, for $n \to \infty$, tends to M in the sense that the greatest distance from points of M_n to M tends to zero. Let δ denote the greatest lower bound of $D[\mathfrak{x}]$ for all such admissible sequences. Then an admissible sequence $\mathfrak{x}_n$ for which

$$D[\mathfrak{x}_n] \to \delta$$

is called a *generalized minimizing sequence*. We obviously have $\delta \leq d$, and we shall see that $\delta = d$.

For the existence proof we start with such a sequence $\mathfrak{y}_n$ and replace it by a generalized minimizing sequence of harmonic vectors as follows: We choose r_n so close to 1 that the piecewise smooth curve $\mathfrak{y}_n(r_n, \theta)$ defined by the parameter θ and called M_n lies within the distance $\epsilon = 1/n$ of M and is linked with H. We then form the harmonic surface $\mathfrak{x}^*_n(u, v)$ which is defined on the boundary C of B by $\mathfrak{x}^*_n(1, \theta) = \mathfrak{y}_n(r_n, \theta)$. This surface spans M_n. Since $D[\mathfrak{x}^*_n] \leq D[\mathfrak{y}_n]$, the $\mathfrak{x}^*_n$ are again a generalized minimizing sequence. Now, since M_n and H are linked, there must exist at least one point u_0, v_0 in B such that $\mathfrak{x}^*_n(u_0, v_0)$ is on H. By a complex linear transformation of B into itself we can throw u_0, v_0 into the origin and obtain a harmonic vector $\mathfrak{x}_n$ with $D[\mathfrak{x}_n] = D[\mathfrak{x}^*_n]$ and with the boundary M_n. We operate now with the new sequence $\mathfrak{x}_n$. $D[\mathfrak{x}_n]$ is uniformly bounded. Hence we can, according to an elementary lemma of potential theory, choose a subsequence for which $\mathfrak{x}_n \to \mathfrak{x}$ uniformly in each concentric circle. The harmonic vector $\mathfrak{x}$ has the point $\mathfrak{x}(0, 0)$ on H. According to the usual reasoning we have

$$D[\mathfrak{x}] \leq \lim D[\mathfrak{x}_n] = \delta, \tag{1}$$

and likewise, for any subdomain of B, e.g., for the circle B': $r \leq 1/2$, we have

$$2\alpha = D_{B'}[\mathfrak{x}] = D_{1/2}[\mathfrak{x}] \leq \liminf D_{1/2}[\mathfrak{x}_n]. \tag{2}$$

By the fundamental convergence theorem on boundary values in I or II the boundary of $\mathfrak{x}$ is on M. Since $\mathfrak{x}(0, 0)$ is at a positive distance from M, it follows that $\mathfrak{x}$ is not constant in B or B'. Hence $\alpha > 0$. We therefore have, for sufficiently large n,

$$D_{1/2}[\mathfrak{x}_n] > \alpha > 0, \tag{3}$$

with α fixed.

If we show that $\mathfrak{x}$ is admissible, then $\mathfrak{x}$ is immediately recognized as the solution, and in addition, since $D[\mathfrak{x}] \leq \delta \leq d$ and $D[\mathfrak{x}] \geq d$, the relation $\delta = d$ is established.

All that remains to be proved—and this is the crucial point in the whole reasoning—is that the boundary of $\mathfrak{x}$ is linked with H. To this end we first mark off the points in B for which $\mathfrak{x}(u, v)$ is on H. Since, according to the convergence theorem in I or II, the boundary of $\mathfrak{x}$ is on M, and hence bounded away from H, there are only a finite number of such "intersections," while the number of these points for $\mathfrak{x}_n$ on the other hand need not be bounded. For a given small ϵ we choose a circle $\rho = r_\epsilon$ which encloses all the intersection points of $\mathfrak{x}$, and such that $\mathfrak{x}(\rho, \theta)$ defines a curve M_ϵ everywhere nearer to M than $\epsilon/4$. We then choose n so large that $|\mathfrak{x}_n(\rho, \theta) - \mathfrak{x}(\rho, \theta)| < \epsilon/4$ and that $\mathfrak{x}_n$ have the same number of intersections for $r < \rho$ as $\mathfrak{x}$. Suppose that the curve $\mathfrak{x}(\rho, \theta)$ is not linked with H. $\mathfrak{x}_n(\rho, \theta)$ would then also not be linked with H. But, since the curve $\mathfrak{x}_n(1, \theta)$ is linked with H, the algebraic sum of the intersection numbers of $\mathfrak{x}_n$ corresponding to the ring $R_\epsilon : \rho < r < 1$ would therefore not vanish.

Now the values $D[\mathfrak{x}_n]$ are equally bounded by a bound A^2. Hence there exists, for each $\mathfrak{x}_n$, a value $\theta = \beta$ such that

$$\frac{1}{2}\int_{1/2}^{1}\left(\frac{\partial \mathfrak{x}_n}{\partial r}\right)^2 dr \leq \int_{1/2}^{1}\left(\frac{\partial \mathfrak{x}_n}{\partial r}\right)^2 r dr < \frac{1}{2\pi}A^2,$$

and hence, by Schwarz's inequality,

$$|\mathfrak{x}_n(r, \beta) - \mathfrak{x}_n(1, \beta)|^2 < (1 - r)\frac{A^2}{\pi}.$$

Hence the oscillation of $\mathfrak{x}_n(r, \beta)$ in the segment S: $\theta = \beta$ for $\rho \leq r \leq 1$ is less than $\epsilon/4$ if ρ is chosen near enough to 1; consequently the values of $\mathfrak{x}_n$ on the segment S are at a distance less than $\epsilon/2$ from M, since $\mathfrak{x}_n(1, \beta)$ is on M. We cut the ring R along S and thus obtain a simply connected domain $R^* = R_\epsilon^*$ whose boundary is mapped by $\mathfrak{x}_n$ on a continuous curve nearer to M than ϵ and linked with H. (No intersection points of $\mathfrak{x}_n$ can correspond to points on S, since such points are farther away from M than ϵ.) We have

$$D_{R^*}[\mathfrak{x}_n] = D[\mathfrak{x}_n] - D_{B-R^*}[\mathfrak{x}_n]$$

and

$$D_{B-R^*}[\mathfrak{x}_n] > D_{1/2}[\mathfrak{x}_n] > \alpha$$

because of (3), hence

$$D_{R^*}[\mathfrak{x}_n] < D[\mathfrak{x}_n] - \alpha$$

If we let ϵ tend to zero and, accordingly, n to infinity and ρ to 1, we have

$$\liminf D_{R^*}[\mathfrak{x}_n] \leq \delta - \alpha. \qquad [4]$$

But, by a conformal mapping R^* can be transformed into the unit circle B and $\mathfrak{x}_n$ in R^* into a vector $\mathfrak{z}_n$ in B with $D[\mathfrak{z}_n] = D_{R^*}[\mathfrak{x}_n]$. The sequence $\mathfrak{z}_n$ is certainly an admissible sequence. Hence

$$\liminf D[\mathfrak{z}_n] = \liminf D_{R^*}[\mathfrak{x}_n] \geq \delta,$$

which contradicts (4). Therefore our assumption that $\mathfrak{x}$ is not admissible is refuted and the existence proof completed.

II. Remarks.—(1) If we consider the special case where M degenerates into a Jordan curve, we obtain by our method the solution of a problem similar to the Plateau problem, but different in so far as a much wider class of surfaces is admitted to competition. But, as stated before in II, this more general problem leads to the same solution as the Plateau problem.[5]

(2) The solution of the variational problem satisfies a natural boundary condition expressing orthogonality in a certain average sense.[6]

(3) The problem and method of this paper lead to a variety of generalizations. We can consider minimal surfaces not only having prescribed topological structure, but also having prescribed linking properties, e.g., prescribed linking numbers of boundary elements with different preassigned cycles linked with homology classes on M. The solution of problems thus specified depends on sufficient conditions in the form of inequalities similar to those known from the Plateau-Douglas problem; and, in addition, inequalities referring to the topological structure of the minimal surface relative to the manifold M. The result in all cases is as follows: A solution of a prescribed topological type with prescribed linking numbers exists if the lower bound for the areas under these conditions is strictly smaller than for other (not necessarily lower) linking numbers and for lower topological type of surfaces.[7]

[1] Courant, "The Existence of a Minimal Surface of Least Area Bounded by Prescribed Jordan Arcs and Prescribed Surfaces," these PROCEEDINGS, **24**, 97 (1938)—hereafter referred to as I.

[2] Courant, "The Existence of Minimal Surfaces of Given Topological Structure under

Prescribed Boundary Conditions," printed in *Acta Math.* and soon to appear. This paper will be referred to as II.

[3] Two simple closed curves C_1, C_2 in the three-dimensional space are said to be "linked" if the algebraic sum of the intersections of C_2 with an orientable surface spanning C_1 (or, vice versa, C_1 with a surface spanning C_2) is different from zero. (See Alexandroff-Hopf, *Topologie*, pp. 413–426.)

[4] This is defined as follows: If $\xi(u, v)$ is represented parametrically in a domain D of the u, v-plane having the boundary C, then the boundary values of ξ are said to be on M if, for every sequence (u_n, v_n) which tends to C, the distance of $\xi(u_n, v_n)$ from M tends to zero.

[5] The proof will be given elsewhere.

[6] See II.

[7] A detailed paper by N. Davids on these questions will be published later.

ON CAUCHY'S INTEGRAL THEOREM AND ON THE LAW OF THE MEAN FOR NON-DERIVABLE FUNCTIONS

BY GUIDO FUBINI

INSTITUTE FOR ADVANCED STUDY

Communicated February 10, 1940

In a recent very interesting paper, printed in these PROCEEDINGS, **25**, 621 (1939), Professor Menger studies a fundamental question. In a rectangle R let $p(x, y)$ and $q(x, y)$ be two continuous functions; we associate with each rectifiable curve C the number $J(C) = \int_C (pdx + qdy)$. Under which condition *is J the same for any coterminal curves in R?* (In other words, under which condition is $pdx + qdy$ an *exact* differential?) It is sufficient to study here the broken lines C, the sides of which are parallel to the x-axis or to the y-axis. Therefore we will only study under which condition the preceding integral is equal to zero, when the path of integration is a rectangle, whose sides are parallel to the axes, for instance, when the path of integration is the boundary of R.

I find here a new simple condition, which is both necessary and sufficient, and add some other simple remarks.

1. With Menger's notations we suppose that R is the rectangle $a \leqslant x \leqslant b$, $c \leqslant y \leqslant d$. If we arbitrarily choose some numbers x_i, y_j such that

$$a = x_0 < x_1 < \ldots\ldots < x_m < x_{m+1} = b,$$

$$c = y_0 < y_1 < \ldots\ldots < y_n < y_{n+1} = d,$$

we will say that the points (x_i, y_j) define a rectangular *net* in R. The rectangle R will be divided into partial rectangles r_{ij}, whose vertices are the points

$$(x_i, y_j), (x_{i+1}, y_j), (x_{i+1}, y_{j+1}), (x_i, y_{j+1}), (i \leqslant m), (j \leqslant n).$$

The sides of this net are the segments joining two points

$$(x_i, y_j) \text{ and } (x_{i+1}, y_j) \text{ or two points } (x_i, y_j), (x_i, y_{j+1}).$$

By changing Menger's definition, we will say that we have *dotted* the net, if we have chosen a point on every side: a point (ξ_{ij}, y_j) on the side joining (x_i, y_j) and (x_{i+1}, y_j) and a point (x_i, η_{ij}) on the side joining the points (x_i, y_j) and (x_i, y_{j+1}). Consequently

$$x_i \leqslant \xi_{ij} \leqslant x_{i+1}; \qquad y_j \leqslant \eta_{ij} \leqslant y_{j+1}. \tag{1}$$

We will consider the ratios

$$\frac{\Delta p}{\Delta y} = \frac{p(\xi_{i,j+1}, y_{j+1}) - p(\xi_{ij}, y_j)}{y_{j+1} - y_j} \tag{2}$$

and

$$\frac{\Delta q}{\Delta x} = \frac{q(x_{i+1}, \eta_{i+1,j}) - q(x_i, \eta_{ij})}{x_{i+1} - x_i} \tag{3}$$

and their *difference*

$$\delta_{ij} = \left| \frac{\Delta p}{\Delta y} - \frac{\Delta q}{\Delta x} \right|.$$

For the sake of simplicity, we will also write

$$p(\xi_{ij}, y_j) = p_{ij}; \; q(x_i, \eta_{ij}) = q_{ij}$$

$$\frac{\Delta p}{\Delta x} = \frac{p_{i,j+1} - p_{ij}}{y_{j+1} - y_j}, \quad \frac{\Delta q}{\Delta y} = \frac{q_{i+1,j} - q_{ij}}{x_{i+1} - x_i}. \tag{4}$$

If we consider other points $\bar{\xi}_{ij}$, $\bar{\eta}_{ij}$ (where $x_i \leqslant \bar{\xi}_{ij} \leqslant x_{i+1}$, and $y_j \leqslant \bar{\eta}_{ij} \leqslant y_{j+1}$), we will write

$$\bar{p}_{ij} = p(\bar{\xi}_{ij}, y_j); \; \bar{q}_{ij} = q(x_i, \bar{\eta}_{ij}). \tag{4bis}$$

We can now state the condition, which is both *necessary* and *sufficient:* If $\epsilon > 0$, $\sigma > 0$ are two positive numbers, arbitrarily small, we can find a dotted net, such that *the lengths of all its sides are less than* ϵ, *and all the differences* δ *are less than* σ.

From the following proof it will appear evident that, in the preceding condition, we might disregard the number σ and say that *all the differences* δ *are equal to zero.*

The condition is necessary: Let us suppose that p, q are arbitrary continuous functions. According to the law of the mean, we can choose the numbers $\bar{\xi}_{ij}$, $\bar{\eta}_{ij}$ in such a way that

$$\int_{x_i, y_j}^{x_{i+1}, y_j} p(x, y)dx = (x_{i+1} - x_i)p(\bar{\xi}_{ij}, y_j) = (x_{i+1} - x_i)\bar{p}_{ij}$$

$$\int_{x_i, y_j}^{x_i, y_{j+1}} q(x, y)dy = (y_{j+1} - y_j)q(x_i, \bar{\eta}_{ij}) = (y_{j+1} - y_j)\bar{q}_{ij}$$

$$(x_i < \bar{\xi}_{ij} < x_{i+1}), \quad (y_j < \bar{\eta}_{ij} < y_{j+1}).$$

We indicate now by $\int_R$ or $\int_r$ the values of the integral of $pdx + qdy$, when the path of integration is the positive boundary of R or of $r = r_{ij}$. And we find immediately that

$$\int_r = -(x_{i+1} - x_i)(\bar{p}_{i,j+1} - \bar{p}_{ij}) + (y_{j+1} - y_j)(\bar{q}_{i+1,} - \bar{q}_{ij}). \quad (5)$$

If $pdx + qdy$ is an exact differential, this integral is equal to zero; and therefore (5) proves that $\delta = 0$, if we choose the dotting points ξ, η, by supposing that $\xi_{ij} = \bar{\xi}_{ij}$, $\eta_{ij} = \bar{\eta}_{ij}$, $(p = \bar{p}, q = \bar{q})$. (Obviously $\delta < \sigma$, since $\delta = 0$.) Before we prove that the condition is also sufficient, it may be useful perhaps to study the differential meaning of the ratios (2) and (3). Let us, for instance, study the former, and let x_i be a constant, while y and $x_{i+1} - x_i = h$ are variable. The point $\bar{\xi}$ such that

$$\int_{x_i}^{x_i+1} p(x, y)dx = hp(\bar{\xi}_{ij}, y) = h\bar{p}_{ij} \quad (6)$$

$$(x_i \leqslant \bar{\xi}_{ij} < x_{i+1} = x_i + h)$$

is a function $\bar{\xi}(y, h)$ of y and h. We can completely determine it, even if there are many points $\bar{\xi}$ satisfying (6); it is sufficient to choose the least; which is possible, because p is continuous. If we suppose that $x = \bar{\xi}$, the function $p(x, y)$ becomes a function $P(h, y)$ of h, y. When y_{j+1} approaches y_j, the ratio (3) approaches the limit

$$\frac{q(x + h, y) - q(x, y)}{h}; \qquad (x = x_i, y = y_j) \qquad (x + h = x_{i+1}) \quad (7)$$

and consequently also the ratio (2), which is equal to (3), approaches the same limit, which is therefore equal to $\dfrac{\partial P}{\partial y}$. (Here $\xi = \bar{\xi}$, $\eta = \bar{\eta}$.)

From what we have already proved we deduce consequently: It may happen that $p(x, y)$ is a non-derivable function of y, when we suppose that $x = \text{const.}$ But *the derivative of p with respect to y exists if* [instead of supposing that $x = \text{const.}$] we suppose that $x = \bar{\xi}(y, h)$. And this derivative is equal to (7).

The condition is sufficient. Let us suppose that $\delta < \sigma$ (for every one of the rectangles $r = r_{ij}$). From (5) we infer that

$$\int_r = A_{ij} - (x_{i+1} - x_i)\{[\bar{p}_{i,j+1} - \bar{p}_{ij}] - [p_{i,j+1} - p_{ij}]\} + \\ + (y_{j+i} - y_j)\{[\bar{q}_{i,j+1} - \bar{q}_{ij}] - [q_{i,j+1} - q_{ij}]\}, \quad (8)$$

where

$$A_{ij} = -(x_{i+1} - x_i)(p_{i,j+1} - p_{ij}) + (y_{j+1} - y_j)(q_{i+1,j} - q_{ij})$$

is deduced from the second member of (5), by writing ξ, η instead of $\bar{\xi}$, $\bar{\eta}$. Since $\delta < \sigma$, we get

$$|A| < \sigma(x_{i+1} - x_i)(y_{j+1} - y_j). \quad (9)$$

We remark, moreover, that, for instance:

$$\sum_j (\bar{p}_{ij} - \bar{p}_{i,j+1}) = \bar{p}_{i0} - \bar{p}_{i,n+1} = p(\bar{\xi}_{i0}, c) - p(\bar{\xi}_{i,n+1}, d). \quad (10)$$

For the sake of brevity, we do not write the analogous equations for p_{ij}, $\bar{q}_{ij}$, q_{ij}. From (9) and (10) we can now immediately deduce that

$$\int_R = \sum \int_r = \sum A_{ij} + \sum_i (x_{i+1} - x_i)[(\bar{p}_{i0} - \bar{p}_{i,n+1}) - \gamma - \\ - (p_{i0} - p_{i,n+1})] + \sum_j (y_{j+1} - y_j)[(\bar{q}_{m+1,} - \bar{q}_{0j}) - (q_{m+1,\bar{j}}\, q_{0j})]. \quad (11)$$

From (9) we deduce that

$$|\Sigma A_{ij}| < \sigma(b - a)(d - c).$$

Since $p(x, c)$ is continuous and therefore integrable, the sum

$$\sum (x_{i+1} - x_i)[\bar{p}_{i0} - p_{i0}] = \sum (x_{i+1} - x_i)[p(\bar{\xi}_i, c) - p(\xi_{i0}, c)] \\ (x_i \leqslant \xi_{i0} \leqslant x_{i+1}) \qquad (x_i \leqslant \bar{\xi}_{i0} < x_{i+1})$$

becomes infinitesimal, when the greatest side of our net approaches zero. In the same way we can study the other terms of the second member of (11). And we prove by this method that $\int_R$ is arbitrarily small, by choosing ϵ and σ sufficiently small. Therefore $\int_R = 0$; which we had to demonstrate.

2. *The Law of the Mean.*—Let us write

$$\int_r = -\int_{x_i}^{x_i+1}[p(y_{j+1}, x) - p(y_j, x)]dx + \int_{y_j}^{y_j+1}[q(x_{i+1}, y) - q(x_i, y)]dy$$

$$x = x_i,\ y_j = y,\ x_{i+1} - x_i = h,\ y_{j+1} - y_j = k.$$

From the equation $\int_r = 0$ we deduce, by using the usual law of the mean for the integrals of the continuous functions

$$p(y_{j+1}, x) - p(y_j, x) \text{ and } q(x_{i+1}, y) - q(x_i, y)$$

that, for every rectangle r, we can find two numbers θ, θ' satisfying the inequalities $0 < \theta < 1$, $0 < \theta' < 1$ such that

$$\frac{p(y + k, x + \theta h) - p(y, x + \theta h)}{k} = \frac{q(x + h, y + \theta' k) - q(x, y + \theta' k)}{h}.$$

The question as to whether this condition is also sufficient is still unanswered.

This condition is equivalent to the law of the mean; by remarking that $\varphi(x + y)(dx + dy)$ is an exact differential, if φ is a continuous function, even if it is not derivable, we deduce a *law of the mean* for the continuous functions $\varphi(z)$, even if they are not derivable. The proof is quite elementary and will be printed in another periodical. I will be contented to state here the final result without demonstration.

If $\varphi(z)$ is continuous in the closed interval $a \leqslant z \leqslant a + H$, we get:

$$\frac{\varphi(a + H) - \varphi(a)}{H} = \frac{\varphi(a + \theta H + h) - \varphi(a + \theta H)}{h}$$

where h is an *arbitrary* sufficiently small number, and (if φ, a, H are given) θ is a function of h with following properties:

α) $0 < \theta < 1$.

β) The point $a + \theta h$ *approaches a limit*, if h becomes infinitesimal.

This law becomes equivalent to the usual law of the mean, if $\varphi(x)$ is a *derivable* function.

3. *Fourier's Coefficients.*—But we can also consider our question from another point of view. If p, q are continuous functions, and $pdx + qdy$ is an exact differential, for instance the function p is not an arbitrary continuous function. This is obvious, because in this case

$$\int_a^b p(x, y)dx \qquad (a, b = \text{const.})$$

must be a function, which possesses a derivative $q(b, y) - q(a, y)$ with respect to y. And when $\varphi(x)$ is a function of x, with a continuous derivative $\varphi'(x)$, also

$$\int_a^b p(x, y)\varphi(x)dx = \left[\varphi(x)\int_a^x p(x, y)dx\right]_{x=a}^{x=b} - \int_a^b \left[\int_a^x p(x, y)dx\right]\varphi'(x)dx$$

is a function of y with a bounded derivative

$$\varphi(b)[q(b, y) - q(a, y)] - \int_a^b [q(x, y) - q(a, y)]\varphi'(x)dx = \varphi(b)q(b, y) - \varphi(a)q(a, y) - \int_a^b \varphi'(x)q(x, y)dx.$$

We deduce, for instance, that, if we consider p as a function of the only variable x, by supposing $y = \text{const.}$, and develop p in a Fourier's series, *its Fourier's coefficient must be derivable functions of* y. The class of functions, which have this property, may perhaps be interesting, but I did not succeed in proving that we can choose $p(x, y)$ arbitrarily in this class of functions.

Let us suppose, for the sake of simplicity, that the length of every side of R is 2π, and that inside R

$$a_0(y) + \sum [a_n(y) \cos nx + b_n(y) \sin nx]$$

is Fourier's development of $p(x, y)$. According to the preceding remark, the coefficients a, b are derivable functions of y. I *believe*, but I could not demonstrate, that (if $pdx + qdy$ is an exact differential) $q(x. y)$ may be defined by the development

$$\phi(y) + xa_0'(y) + \sum\left[a_n'(y)\frac{\sin nx}{n} + b_n'(y)\frac{1 - \cos nx}{n}\right]$$

where $\phi(y)$ is an arbitrary integrable function of y. If x, y were polar coordinates, and y were the radius vector, the formulas become simpler, because necessarily a_0 is equal to zero (at least if $pdx + qdy$ is the differential of an one-valued function and the origin belongs to the considered region).

RECALCULATION AND EXTENSION OF THE MODULUS AND OF THE LOGARITHMS OF 2, 3, 5, 7 AND 17

BY HORACE S. UHLER

SLOANE PHYSICS LABORATORY, YALE UNIVERSITY

Communicated February 1, 1940

A year or more ago while the author was engaged in extending the work of J. C. Adams[1] by computing the Napierian logarithms of 11, 13, 17, 19, 23, 29 and 31 to a fairly large number of decimal places, but before the calculations had been completed, he became convinced that it would not be justifiable to claim for the new values complete absence of error unless the basic data, namely, the logarithms of 2, 3, 5 and 7, were proved to be correct as printed. This conclusion was reached after a careful search through the available literature failed to show that in the interim any other mathematician had repeated or independently verified the values found by Adams. In order to contribute more than the mere checking of the classical data the goal of nearly 330 decimal places was set for the present investigation. Since Adams' approximations were claimed by him to be valid to about 273 decimal places the gain proposed would be 55 figures.

The notation used here is the same as that employed by me in an earlier paper.[2] The actual work involved the following steps in the order stated: (*a*) the selection of suitable pairs of numbers (p, q) which satisfy the condition $p - q = 1$; (*b*) the calculation of terms of the simple geometrical series $\Sigma(2p-1)^{-(2m+1)}$, $m = 0, 1, 2, 3, \ldots$; (*c*) copying from the Monroe computing machine (in black ink) the numerical values of these terms on alternate horizontal lines of rectangularly ruled paper; (*d*) forming the sum of these data and comparing it with the previously computed value of S_∞, that is, the limit $(2p-1)/4p(p-1)$; (*e*) dividing each value of $(2p-1)^{-(2m+1)}$ by $2m+1$ and entering the quotients (in red ink) in the blank lines directly below the corresponding terms of the geometrical series; (*f*) summing separately the lines which represent the even and odd terms of the final series, $s(+) = \sum_0 (2p-1)^{-(4m+1)}/(4m+1)$ and $s(-) = \sum_1 (2p-1)^{-(4m-1)})/(4m-1)$; and (*g*) evaluation of $\log (p/q)$ and $\tan^{-1}[1/(2p-1)]$, respectively, as $2[s(+) + s(-)]$ and $s(+) - s(-)$. All quotients were checked by multiplication, the results of addition were tested by repetition with the successive groups of ten figures staggered five decimal places, and throughout all stages of the work every precaution known to me was taken to eliminate errors.

The pairs of numbers chosen for the calculation of the logarithms l_2, l_3, l_5, l_7 and l_{17} are given in table 1.

TABLE 1

$2p-1$	p	q
5	3	2
239	$120 = 2^3 \cdot 3 \cdot 5$	$119 = 7 \cdot 17$
577	$289 = 17^2$	$288 = 2^5 \cdot 3^2$
2449	$1225 = 5^2 \cdot 7^2$	$1224 = 2^3 \cdot 3^2 \cdot 17$
4999	$2500 = 2^2 \cdot 5^4$	$2499 = 3 \cdot 7^2 \cdot 17$
8749	$4375 = 5^4 \cdot 7$	$4374 = 2 \cdot 3^7$

The selection of these particular numbers was based not only upon the essential condition that they should have the prime factors 2, 3, 5 and 7 but also upon other considerations. For example, 5 and 239 lead to $\tan^{-1}(1/5)$ and $\tan^{-1}(1/239)$, that is, to numbers which can be checked either directly and separately by comparison with the values calculated by Rutherford[3] and Shanks[4] or indirectly and collectively with the standard value of π through Machin's formula. The choice of $2p - 1 = 239$ or $q = 7 \cdot 17$ obviously introduced the number 17 into the work. Since $(2449)^2 = 5997601 = 6 \times 10^6 - 2 \times 10^3 - 4 \times 10^2 + 1 \times 10^0$ the quotients constituting the terms of the geometrical series of which $1/(2449)^2$ is the common ratio can be checked rapidly by multiplication. In fact the number of unit strokes of the computing machine in this case is only 13 $(= 6 + 2 + 4 + 1)$. Similarly $(4999)^2 = 24990001 = 2 \times 10^7 + 5 \times 10^6 - 1 \times 10^4 + 1 \times 10^0$ which requires only 9 strokes for every ten consecutive digits in the quotient.

For brevity let $a_1 = S(1/5)$, $a_2 = S(1/239)$, $a_3 = S(1/2449)$, $a_4 = S(1/4999)$ and $a_5 = S(1/8749)$. Then the required logarithms are given by the following set of independent linear equations:

$$\left.\begin{aligned} -1l_2 + 1l_3 &= 2a_1 \\ 3l_2 + 1l_3 + 1l_5 - 1l_7 - 1l_{17} &= 2a_2 \\ -3l_2 - 2l_3 + 2l_5 + 2l_7 - 1l_{17} &= 2a_3 \\ 2l_2 - 1l_3 + 4l_5 - 2l_7 - 1l_{17} &= 2a_4 \\ -1l_2 - 7l_3 + 4l_5 + 1l_7 &= 2a_5 \end{aligned}\right\}. \qquad (1)$$

These equations are satisfied identically by the expressions:

$$\left.\begin{aligned} l_2 &= (\ 27a_1 + 18a_2 - \ 7a_3 - 11a_4 + 10a_5)/8 \\ l_3 &= (\ 43a_1 + 18a_2 - \ 7a_3 - 11a_4 + 10a_5)/8 \\ l_5 &= (\ 63a_1 + 26a_2 - 11a_3 - 15a_4 + 18a_5)/8 \\ l_7 &= (\ 76a_1 + 40a_2 - 12a_3 - 28a_4 + 24a_5)/8 \\ l_{17} &= (111a_1 + 42a_2 - 27a_3 - 31a_4 + 34a_5)/8 \end{aligned}\right\}. \qquad (2)$$

In each of the preceding parentheses the coefficients of a_1 and a_2 are larger than those of a_3, a_4 and a_5 wherefore a_1 and a_2 were calculated to 336 and 335 decimal places, respectively, while the three remaining a's were rounded off at the 330th place.

After the l's had been computed from formulas (2) the values obtained were found by substitution to satisfy equations (1) as far as and beyond the 333d decimal place. This agreement merely means that no mistake was made while substituting the numbers in formulas (2) and it would have been obtained even if one or more of the a's and the dependent l's were vitiated by errors. Hence the necessity for discovering if possible an identity which could only be fulfilled by a set of perfect a's became imperative.

An exhaustive inspection of the British Association Factor Table[5] from 1 to 50,000 (that is, throughout the range of numbers whose squares did not exceed the capacity of the computing machines employed) showed that (289, 288) is the largest pair of consecutive integers which fulfil the following conditions: (i) one member of the pair shall be a multiple of 17; (ii) all the remaining prime factors of the pair shall be comprised in the group 1, 2, 3, 5 and 7; (iii) the pair must lead to an equation which, when combined with equations (1) will give an identity connecting *all* of a_1, a_2, a_3, a_4 and a_5. Since $289 = 17^2$ and $288 = 2^5 \cdot 3^2$ the equation in question is

$$-5l_2 - 2l_3 + 2l_{17} = 2a_6 \tag{3}$$

where $a_6 = S(1/577)$, and the analytical condition for the compatibility of the six equations is the required identity, namely

$$a_1 - 42a_2 - 5a_3 + 15a_4 - 2a_5 - 16a_6 = 0. \tag{4}$$

This formula can also be obtained by equating the logarithms of both sides of the following identity the truth of which can be tested at once by replacing the composite numbers by their prime factors as given in table 1.

$$\left(\frac{3}{2}\right)^{-1}\left(\frac{120}{119}\right)^{42}\left(\frac{1225}{1224}\right)^{5}\left(\frac{2500}{2499}\right)^{-15}\left(\frac{4375}{4374}\right)^{2}\left(\frac{289}{288}\right)^{16} = 1. \tag{5}$$

Incidentally the smaller pair of numbers ($p = 256 = 2^8$, $q = 255 = 3 \cdot 5 \cdot 17$) leads to the alternative identity

$$a_1 - 58a_2 + 11a_3 + 31a_4 - 18a_5 + 16a_7 = 0 \tag{6}$$

in which $a_7 = S(1/511)$ converges even more slowly than $S(1/577)$. With reference to rate of convergence the fact may merit recording that in order to increase the number of decimal places for $S(1/577)$ from 273 to 328—a gain of about 20 per cent—it was necessary to augment by over 51 per cent the number of figures actually written in the terms of the series.

Attention will now be turned to the quantitative evidence for the degree of accuracy both of the final data published by J. C. Adams and of the numbers involved at various stages in the present work. The "errors" in Adams' constants are entirely terminal and they are given in table 2.

TABLE 2

CONSTANT	ERROR
log 2	$+4.43 \times 10^{-275}$
log 3	$+6.95 \times 10^{-275}$
log 5	$+1.01 \times 10^{-274}$
log 7	$+1.44 \times 10^{-274}$
log 10	$+1.45 \times 10^{-274}$
M	-9.46×10^{-273}

It is interesting to note that all of his logarithms have errors of the same sign. With characteristic perspicacity Adams[6] wrote "And finally the corrected value of the Modulus is $M = 0.43429 \ldots 21868\ 25$ which is true, certainly to 272 and probably to 273 places of decimals."

The geometrical series test yielded the first six of the equations transcribed below. It was not applied to the functions of $1/5$ $(= 2 \times 10^{-1})$ since their evaluation depended explicitly upon positive integral powers of 2. These involutions had been thoroughly verified by the writer in the year 1900.

$$+S_\infty(1/239) - \sum_0^{34}(239)^{-(4m+1)} = 1.6 \times 10^{-335} \qquad S_\infty(1/2449) - \sum_0^{48}(2449)^{-(2m+1)} = 3.6 \times 10^{-330}$$

$$-S_\infty(1/239) - \sum_1^{35}(239)^{-(4m-1)} = 1.2 \times 10^{-335} \qquad S_\infty(1/4999) - \sum_0^{44}(4999)^{-(2m+1)} = 1.3 \times 10^{-330}$$

$$S_\infty(1/577) - \sum_0^{60}(577)^{-(2m+1)} = 2.0 \times 10^{-335} \qquad S_\infty(1/8749) - \sum_0^{41}(8749)^{-(2m+1)} = 3.0 \times 10^{-330}$$

$$[\tan^{-1}(1/5)]_S - [\tan^{-1}(1/5)]_U = 4.0 \times 10^{-336}.$$

$$[\tan^{-1}(1/239)]_S - [\tan^{-1}(1/239)]_U = -1.6 \times 10^{-335}.$$

$$\pi_S - \pi_U = 1.3 \times 10^{-334}.$$

The subscripts S and U refer to Shanks and Uhler, respectively.

Substitution of the newly extended values of l_2, l_3 and l_{17} in equation (3), a relation which was not used in the calculation of these logarithms, led to the following significant result:

$$2l_{17} - 5l_2 - 2l_3 - 2a_6 = 4.05 \times 10^{-331}.$$

The left-hand member of the important identity (4) was evaluated to be 3.2×10^{-330}. This admissible error is ascribable solely to the trinomial $15a_4 - 5a_3 - 2a_5$ since each of a_1, a_2 and a_6 was carried as far as the 335th decimal place while a_3, a_4 and a_5 were rounded off at the 330th place. Fi-

nally in checking the value of the modulus by forming the product $M \cdot l_{10}$ a continuous succession of 336 nines was obtained.

The newly extended values of the natural logarithms of 2, 3, 5, 7 and 17, and of the common modulus are collected in table 3. These approximations are certainly correct to 328 decimal places and their unreliability probably does not exceed one or two units in the 329th place. If at any future time the values of the discrete sums of the positive and negative terms of the infinite series involved in the present work should be desired they may be obtained directly by first calculating the a's through substitution of the tabulated l's in equations (1) and then employing the following formulas:

$$\left.\begin{aligned} s_j(+) &= (a_j + \tan^{-1}\theta_j)/2 \\ s_j(-) &= (a_j - \tan^{-1}\theta_j)/2 \end{aligned}\right\}. \tag{7}$$

In addition to the arc tangents of the reciprocals of the integers 577, 2449, 4999 and 8749 table 3 gives the values of $\tan^{-1}(1/451)$ and $\tan^{-1}(1/10081)$, and also the extensions of certain other constants which were published by me in an earlier paper.[7] These two arc tangents have just been computed from the series underlying, respectively, the values of log 113 and log 71 which were used in calculating log π from Ramanujan's expression.[2] The extensions were finished on May 18, 1937, while retesting a table of reciprocals of factorials. They are printed in table 3 in such a manner as to fit and continue the corresponding numbers as printed on pages 433 and 434 of the monograph[7] in question. The accuracy of the extended numbers is measured by the right-hand members of the following test equations:

$$1 - (e^{-10}) \times (e^{+10}) = 5.0 \times 10^{-295},$$

$$\cos^2 10 + \sin^2 10 - 1 = 4.3 \times 10^{-288}.$$

TABLE 3

$\log_e 2 =$

0.69314	71805	59945	30941	72321	21458	17656	80755	00134	36025
52541	20680	00949	33936	21969	69471	56058	63326	99641	86875
42001	48102	05706	85733	68552	02357	58130	55703	26707	51635
07596	19307	27570	82837	14351	90307	03862	38916	73471	12335
01153	64497	95523	91204	75172	68157	49320	65155	52473	41395
25882	95045	30070	95326	36664	26541	04239	15781	49520	43740
43038	55008	01944	17064	16715	18644				

TABLE 3 (*Continued*)

$\log_e 3 =$

1.09861 22886 68109 69139 52452 36922 52570 46474 90557 82274
94517 34694 33363 74942 93218 60896 68736 15754 81373 20887
87970 02906 59578 65742 36800 42259 30519 82105 28018 70767
27741 06031 62769 18338 13671 79373 69884 43609 59903 74257
03167 95911 52114 55919 17750 67134 70549 40166 77558 02222
03170 25294 68975 60690 10652 15056 42868 13803 63173 73298
57778 23669 91654 79213 18181 49019 5

$\log_e 5 =$

1.60943 79124 34100 37460 07593 33226 18763 95256 01354 26851
77219 12647 89147 41789 87707 65776 46301 33878 09317 96107
99966 30302 17155 62899 72400 52293 24676 19963 36166 17463
70572 75521 79637 49718 32456 53492 85620 23415 25057 27015
51936 00879 77738 97256 88193 54071 27661 54731 22180 95279
48521 29282 13580 59722 56767 22852 87240 46158 94481 78364
67132 86739 98424 63775 95931 89422

$\log_e 7 =$

1.94591 01490 55313 30510 53527 43443 17972 96370 84729 58186
11884 59390 14993 75798 62752 06926 77876 58498 58787 15269
93061 69420 58511 40911 72375 22576 77786 84314 89580 95163
90077 59078 24468 10427 47833 82259 34900 84673 74412 50497
37048 53551 76783 55774 86240 15102 77418 08868 67107 51412
13480 93879 74183 10810 25182 31684 93014 07330 63932 87711
93411 21406 87692 40026 05769 35850

$\log_e 10 =$

2.30258 50929 94045 68401 79914 54684 36420 76011 01488 62877
29760 33327 90096 75726 09677 35248 02359 97205 08959 82983
41967 78404 22862 48633 40952 54650 82806 75666 62873 69098
78168 94829 07208 32555 46808 43799 89482 62331 98528 39350
53089 65377 73262 88461 63366 22228 76982 19886 74654 36674
74404 24327 43651 55048 93431 49393 91479 61940 44002 22105
10171 41748 00368 80840 12647 08066

$\log_e 17 =$

2.83321 33440 56216 08024 95346 17873 12653 55882 03012 58574
47872 97237 73788 22925 75800 93128 09120 94868 03750 29475
18348 26204 71870 57291 39759 28419 46738 36429 97545 65742
02127 12599 13208 07209 04790 76471 68172 51666 60296 60850
69091 96813 96134 51492 95164 19209 44718 69393 25481 33184
68944 45037 58003 15646 02993 05896 37270 00327 36297 59273
99414 82424 46984 21556 64224 34393 5

TABLE 3 (*Continued*)

$M =$

0.43429 44819 03251 82765 11289 18916 60508 22943 97005 80366
65661 14453 78316 58646 49208 87077 47292 24949 33843 17483
18706 10674 47663 03733 64167 92871 58963 90656 92210 64662
81226 58521 27086 56867 03295 93370 86965 88266 88331 16360
77384 90514 28443 48666 76864 65860 85135 56148 21234 87653
43543 43573 17253 83562 22813 95603 04864 66523 66095 53937
73561 76323 43191 67109 91411 59790

$\tan^{-1}(1/451) =$

0.00221 72912 66532 02363 15882 56080 23026 31380 14502 60599
17643 99214 52019 13338 55404 43675 39034 82558 58543 44395
87108 04995 88910 09632 24025 89247 92233 60230 24247 94571
84451 16722 83161 33503 39386 54494 07932 77708 39014 76315
64780 05094 35952

$\tan^{-1}(1/577) =$

0.00173 31005 17828 99690 63239 26177 82620 68511 14980 78800
59327 89382 35699 57691 52385 74935 80734 22847 93358 70598
96356 61775 68614 26967 56613 21839 35078 77394 53724 71418
35572 52796 24166 64413 86399 69167 26081 27592 39196 59869
64098 11494 99282 54992 61438 31419 33135 35109 63451 57505
18848 56578 01725 67976 90962 00362 69313 12814 02928 71699
62913 81132 13787 97716 84343 90302 82074

$\tan^{-1}(1/2449) =$

0.00040 83299 07889 84408 18481 31992 99044 00572 06737 74283
70053 38677 45144 46042 13461 35015 77405 60982 70932 45713
04305 99949 52406 66320 25439 93760 94545 22519 84677 64435
46704 46028 26736 37875 65360 61246 63820 16585 22183 67056
63190 96352 77188 35207 98027 61056 13926 78570 20865 44049
90325 26335 10182 52182 64165 03332 27936 85681 33796 89799
93579 54457 16861 92622 49627 60087

$\tan^{-1}(1/4999) =$

0.00020 00400 05333 33307 72479 85371 42948 19785 33228 97143
44926 08256 32095 52603 39634 32975 44539 51845 47049 06238
12923 63094 42014 32150 25583 78435 98399 16704 85072 75018
36338 02163 03169 96623 07518 40270 67119 84057 80148 26486
18610 47735 14108 65609 41020 87318 86948 59472 63931 90140
76445 02147 90530 51061 43414 50219 10796 83471 52085 58089
23900 19074 14132 95931 36220 37343

TABLE 3 (*Continued*)

$\tan^{-1}(1/8749) =$

0.00011	42987	76505	34497	95406	31656	54433	41572	51039	85186
41170	24388	58112	13047	19377	06999	98474	56827	20239	77036
33365	59321	49574	74236	74070	56118	40358	72195	87487	08290
49969	68785	15908	88360	69720	37795	09205	49310	96750	43861
88677	13495	77313	59992	87031	98770	47933	54594	09620	68560
46114	23999	91470	93199	28975	69236	59373	30949	05572	24245
82449	35001	00294	79698	27092	87283				

$\tan^{-1}(1/10081) =$

0.00009	91965	07957	54564	03985	58797	77424	49951	60255	89946
71090	71455	59679	31811	67097	06143	17935	78474	20733	28137
34792	26162	76152	55449	53213	52046	37462	68193	60929	54513
84052	28071	43737	07353	98497	65534	94325	10747	50921	23363
62373	56664	62704	6						

$e^{+10} =$

.....	...07	54381	79319	60834	04440	49342	3668(2)

$e^{-10} =$

....	...30	56049	41570	10772	99753	54408	07940	399(4)

$\sin 10 =$

.....	.....	..290	61127	67064	51048	48711	04571	26379	41468
21392	89420	87572	08458	35061	96715	0157(	96)		

$\cos 10 =$

.....	.....	..471	69711	71010	52082	69213	07324	18341	25670
72265	61830	11009	31356	14920	90281	4223(	32)		

$\cos 20 =$

.....	.....	..197	39399	70438	94194	84010	91837	43935	51103
56225	20596	81042	71693	29701	02133	9639(	40)		

[1] J. C. Adams, *Proc. Roy. Soc. London*, **42**, 22–25 (1887).
[2] H. S. Uhler, *Proc. Nat. Acad. Sci.*, **24**, 23–30 (1938).
[3] Wm. Rutherford, *Proc. Roy. Soc. London*, **6**, 274, 275 (1853).
[4] Wm. Shanks, *Proc. Roy. Soc. London*, **21**, 319 (1873).
[5] *Brit. Assoc. Adv. Sci., Math. Tables*, **5** (1935).
[6] *Scientific Papers of John Couch Adams*, **1**, 470 (1896).
[7] H. S. Uhler, *Trans. Conn. Acad. Arts Sci.*, **32**, 381–434 (1937).

THE GREEN'S FUNCTION FOR A DIFFERENTIAL SYSTEM OF INFINITE ORDER

BY D. V. WIDDER

DEPARTMENT OF MATHEMATICS, HARVARD UNIVERSITY

Communicated February 1, 1940

In the study of the Stieltjes transform[1]

$$f(x) = \int_0^\infty \frac{\varphi(t)}{x+t}\,dt \tag{1}$$

the author was led to consider a certain linear differential operator of infinite order

$$L[f(x)] = \lim_{k\to\infty} \frac{(-1)^{k-1}}{k!(k-2)!}\,[x^{2k-1}f^{(k-1)}(x)]^{(k)}. \tag{2}$$

It was found that when this operator is applied to the function $f(x)$, defined by (1), it yields $\varphi(x)$ and thus inverts the integral (1). It is easily seen that (2) is formally equivalent to[2]

$$L[f(x)] = xD \prod_{n=-\infty}^{\infty}{}' \left(1 - \frac{xD}{n}\right) f(x), \tag{3}$$

where D indicates differentiation with respect to x and the prime indicates that the factor corresponding to $n = 0$ is omitted.

Consider now the following differential system

$$\begin{aligned} L[f(x)] &= \varphi(x) \\ \lim_{x\to 0+} xf(x) &= 0 \\ \lim_{x\to\infty} f(x) &= 0 \end{aligned} \tag{A}$$

and the corresponding homogeneous system (B) in which $\varphi(x)$ is replaced by zero. A fundamental system of solutions of the equation

$$L[f(x)] = 0$$

is

$$f(x) = x^n \qquad (n = 0, \pm 1, \pm 2, \ldots).$$

No linear combination of these solutions satisfies the boundary conditions of (B). Hence (B) is incompatible. That is, (A) has a unique solution. Following the analogy with systems of finite order we should be able to find the solution by use of a Green's function.

Consider now the "truncated" systems (A') and (B') which are the same as (A) and (B), respectively, except that $L[f(x)]$ has been replaced by

$$L_k[f(x)] = -xD \prod_{n=-k}^{k-2} \left(1 - \frac{xD}{n}\right) f(x).$$

We recall that the Green's function[3] $G_k(x, t)$ for the system (A') is for each positive t a function of x which satisfies (B') for every positive x except $x = t$, which is continuous with its first $(2k - 3)$ derivatives for $(0 < x < \infty)$, and whose $(2k - 2)$th derivative is continuous there except at $x = t$, where it has a finite jump defined by the equation

$$\lim_{x \to t+} \frac{\partial^{2k-2}}{\partial x^{2k-2}} G_k(x, t) - \lim_{x \to t-} \frac{\partial^{2k-2}}{\partial x^{2k-2}} G_k(x, t) = (-1)^{k-1} k!(k-2)! t^{-2k+1}.$$

It may be shown that these properties serve to characterize $G_k(x, t)$ and that the solution $f_k(x)$ of (A') is

$$f_k(x) = \int_0^\infty G_k(x, t)\varphi(t)dt.$$

It is natural to define the Green's function $G(x, t)$ of the system (A) as the limit as k becomes infinite of $G_k(x, t)$ and to expect that the solution of (A) will be

$$f(x) = \int_0^\infty G(x, t)\varphi(t)dt. \tag{4}$$

We show that this conjecture is correct.

We can in fact obtain an explicit formula for $G_k(x, t)$. It is found to be

$$G_k(x, t) = k \int_0^\infty \frac{(y + x - t)^{k-1} y^{k-2}}{(y + x)^{2k-1}} dy \qquad (t < x)$$

$$= k \int_0^\infty \frac{(y + t - x)^{k-2} y^{k-1}}{(y + t)^{2k-1}} dy \qquad (t > x).$$

The details of computation will be given in a later paper. Now by the Laplace method for the asymptotic evaluation of an integral, or otherwise, it may be shown that

$$\lim_{k \to \infty} G_k(x, t) = (x + t)^{-1},$$

so that the solution of (A) in the form (4) is precisely (1). That (1) actually satisfies the system (A) was proved in an earlier paper, as we observed at the beginning of this note. Thus the Stieltjes kernel may be regarded as the Green's function for a certain differential system of infinite order.

The importance of the present procedure is that it provides a straightforward method of finding the kernel that corresponds to a given differential operator. As other examples we note that if (A) is altered by omitting[4] the factor $(1 + xD)$ in (3) the kernel becomes $t(x + t)^{-2}$; if in addition the factor $1 + 2^{-1}xD$ is omitted the kernel becomes $t^2(x + t)^{-3}$, etc. If the system (A) is altered by replacing $L[f(x)]$ by its iterate $L^2[f(x)]$ we find that the Green's function for the corresponding truncated system is

$$\int_0^\infty G_k(x, y)G_k(y, t)dy$$

and that the Green's function for the system of infinite order is $[\log(x/t)]$ $[x - t]^{-1}$, as one would expect from earlier consideration of R. P. Boas[5] and the author.

[1] D. V. Widder, "The Stieltjes Transform," *Trans. Am. Math. Soc.*, **43**, 7–60 (1938).

[2] If an exponential change of variable is made (3) is related to a differential operator of the type discussed by J. F. Ritt, "On a General Class of Linear Homogeneous Equations of Infinite Order with Constant Coefficients," *Trans. Am. Math. Soc.*, **18**, 27–49 (1917).

[3] See, for example, M. Bôcher, *Leçons sur les méthodes de Sturm*, Paris (1917), Chap. V.

[4] This leads to the operator $M_{k,t}[f(x)]$ defined on p. 55 of the author's paper cited above. The operator was there seen to correspond with the kernel $t/(x + t)^2$.

[5] R. P. Boas, Jr., and D. V. Widder, "The Iterated Stieltjes Transform," *Trans. Am. Math. Soc.*, **45**, 1–72 (1939).

THEOREMS IN THE INVERSE PROBLEM IN THE CALCULUS OF VARIATIONS

BY JESSE DOUGLAS

BROOKLYN, N. Y.

Communicated January 15, 1940

1. *Introduction.*—In a recent issue of these PROCEEDINGS the author has announced and presented the essential features of a solution of the inverse problem of the calculus of variations recently found by him.[1] This problem is: *Given a curve family, $y_i'' = F_i(x, y_j, y_j')$, $(i, j = 1, \ldots, n)$, in $(n + 1)$-dimensional space; to find, if existent, a variation problem, $\int \varphi(x, y_j, y_j')dx = min.$, having this curve family as the totality of its extremals.*

A fully detailed account of our solution will appear in one of the mathematical journals. The present note summarizes the results of this detailed paper, which it is here our purpose to state.

We have given in our forthcoming paper a general method applying to an $(n + 1)$-dimensional space, and then carried out this plan completely

for the most important and interesting case of 3 dimensions. This results in a classification of all families $\mathfrak{F}$ of ∞^4 curves in xyz-space:

$$y'' = F(x, y, z, y', z'), \qquad z'' = G(x, y, z, y', z'), \tag{1.1}$$

into extremal and non-extremal, together with a determination in the former case of the degree of generality, i.e., the number of arbitrary functions and constants, involved in the corresponding variation problem

$$\int \varphi(x, y, z, y', z')dx = \text{min.} \tag{1.2}$$

Illustrative examples for all the more important cases are given at the end of this note. These are more completely described in our detailed paper.

In stating our results, the following notation introduced by E. Kasner in his review of Riquier's treatise on differential systems[2] is found useful:

$$\infty^{m_1 f(n_1)} + \ldots + m_k f(n_k) \tag{1.3}$$

denotes an infinitude involving m_1 arbitrary functions of n_1 arguments, ..., m_k arbitrary functions of n_k arguments. This extends the classic notation ∞^m for an infinitude involving m arbitrary constants.

All functions occurring in our work are supposed to be *analytic*.

2. *The Matrix* Δ.—We define the following symbols, functions of x, y, z, y', z', whose values are known when the curve family $\mathfrak{F}$ or (1.1) is given.

$$A = \frac{d}{dx}F_{z'} - 2F_z - \frac{1}{2}F_{z'}(F_{y'} + G_{z'}),$$

$$B = -\frac{d}{dx}F_{y'} + \frac{d}{dx}G_{z'} + 2(F_y - G_z) + \frac{1}{2}(F_{y'} - G_{z'})(F_{y'} + G_{z'}),$$

$$C = -\frac{d}{dx}G_{y'} + 2G_y + \frac{1}{2}G_{y'}(F_{y'} + G_{z'}). \tag{2.1}$$

d/dx denotes the operator

$$\frac{d}{dx} \equiv \frac{\partial}{\partial x} + y'\frac{\partial}{\partial y} + z'\frac{\partial}{\partial z} + F\frac{\partial}{\partial y'} + G\frac{\partial}{\partial z'}, \tag{2.2}$$

representing total differentiation as to x along an arbitrary curve of the given family (1.1).

From A, B, C we derive A_1, B_1, C_1 by the following formulas:

$$A_1 = \frac{dA}{dx} - F_{y'}A - \frac{1}{2}F_{z'}B,$$

$$B_1 = \frac{dB}{dx} - G_{y'}A - \frac{1}{2}(F_{y'} + G_{z'})B - F_{z'}C,$$

$$C_1 = \frac{dC}{dx} - \frac{1}{2}G_{y'}B - G_{z'}C; \tag{2.3}$$

while A_2, B_2, C_2 are derived from A_1, B_1, C_1 by the same formulas.

Our results depend to a large extent on the rank of the matrix

$$\Delta \equiv \begin{Vmatrix} A & B & C \\ A_1 & B_1 & C_1 \\ A_2 & B_2 & C_2 \end{Vmatrix}. \tag{2.4}$$

For instance, it is at least a necessary condition for an extremal family that the determinant of this matrix be equal to zero. By non-satisfaction of this condition, therefore, examples of non-extremal families can be constructed at pleasure.

We begin, consequently, with a classification into cases according to the rank of Δ, which will be followed by the appropriate sub-classifications in the statement of our theorems.

Case I: $\begin{Vmatrix} A & B & C \end{Vmatrix} = 0$; i.e., $A = 0, B = 0, C = 0$.

Case II: $\begin{Vmatrix} A & B & C \\ A_1 & B_1 & C_1 \end{Vmatrix} = 0, \begin{Vmatrix} A & B & C \end{Vmatrix} \neq 0.$

Case III: $\begin{vmatrix} A & B & C \\ A_1 & B_1 & C_1 \\ A_2 & B_2 & C_2 \end{vmatrix} = 0, \begin{Vmatrix} A & B & C \\ A_1 & B_1 & C_1 \end{Vmatrix} \neq 0.$

Case IV: $\begin{vmatrix} A & B & C \\ A_1 & B_1 & C_1 \\ A_2 & B_2 & C_2 \end{vmatrix} \neq 0.$

Here, in writing a matrix $= 0$ we mean that each determinant resulting from it by the suppression of columns only is equal to zero, and $\neq 0$ means that at least one such determinant is not equal to zero.

By the recursion formulas (2.3) it is seen that the cases thus described are precisely those of rank 0, 1, 2, 3 of the matrix Δ, respectively.

3. *The Fundamental Differential System S.*—As we prove in our main paper, the solution of the inverse problem of the calculus of variations for the given curve family (1.1) is equivalent exactly to the solution of the following linear differential system, S, for the unknown functions L, M, N of x, y, z, y', z':

$$\frac{dL}{dx} + F_{y'}L + G_{y'}M = 0,$$

$$\frac{dM}{dx} + \frac{1}{2}F_{z'}L + \frac{1}{2}(F_{y'} + G_{z'})M + \frac{1}{2}G_{y'}N = 0,$$

$$\frac{dN}{dx} + F_{z'}M + G_{z'}N = 0;$$

$$AL + BM + CN = 0;$$

$$L_{z'} = M_{y'},\ N_{y'} = M_{z'};$$

$$LN - M^2 \neq 0. \tag{3.1}$$

4. *The "Critical Cone."*—The *inequation* (3.1_7), last relation of the system S, is very important. Its negation,

$$LN - M^2 = 0, \tag{4.1}$$

defines a quadric cone in an auxiliary LMN-space, whose significance first appears in our work on the inverse problem, and which we call the "*critical cone*," denoting it by $\mathfrak{K}$.

The purely algebraic equation (3.1_4) of the differential system, S:

$$AL + BM + CN = 0, \tag{4.2}$$

defines a plane $\mathfrak{P}$ in the LMN-space passing through the vertex of the critical cone, located at the origin. In the discussion of Case II—which is the most interesting and varied in its results—much depends on whether the plane $\mathfrak{P}$ intersects the critical cone $\mathfrak{K}$ in two distinct generators (real or conjugate imaginary) or, on the other hand, is tangent to this cone.

The intersection of $\mathfrak{P}$ with $\mathfrak{K}$ is determined by the quadratic equation

$$A\xi^2 + B\xi + C = 0, \tag{4.3}$$

whose roots, known functions of x, y, z, y', z', will be denoted by λ, μ. Accordingly, we make the following subdivision of Case II:

Case IIa: $B^2 - 4AC \neq 0$, or $\lambda \neq \mu$;

Case IIb: $B^2 - 4AC = 0$, or $\lambda = \mu$.

In Case IIa the following symbols intervene in the statement of our results, where the importance of the hypothesis $\lambda \neq \mu$ is seen in the presence of $\lambda - \mu$ in various denominators.

$$\alpha = \frac{\lambda\lambda_{z'} - \lambda_{y'}}{\lambda - \mu}, \quad \beta = \frac{\mu\mu_{z'} - \mu_{y'}}{\lambda - \mu},$$

$$H = \frac{1}{2} F_{z'}\lambda^2 - \frac{1}{2}(F_{y'} - G_{z'})\lambda - \frac{1}{2}G_{y'},$$

$$I = \lambda_z + H_{z'} - R,$$

$$J = \frac{(H - P)\beta + K}{\lambda - \mu},$$

$$K = \mu\mu_z - \mu_y + P\mu_{z'} - \mu P_{z'} + P_{y'},$$

$$P = \frac{1}{2}F_{z'}\mu^2 - \frac{1}{2}(F_{y'} - G_{z'})\mu - \frac{1}{2}G_{y'},$$

$$Q = \mu_z + P_{z'} - J,$$

$$R = -\frac{(H - P)\alpha + S}{\lambda - \mu},$$

$$S = \lambda\lambda_z - \lambda_y + H\lambda_{z'} - \lambda H_{z'} + H_{y'}. \tag{4.4}$$

In Case II*b* the following symbols are important:[3]

$$\text{(I)} = \frac{1}{2}F_{z'}\lambda^2 - \frac{1}{2}(F_{y'} - G_{z'})\lambda - \frac{1}{2}G_{y'},$$

$$\text{(II)} = F_{z'}\lambda - \frac{1}{2}(F_{y'} - G_{z'}),$$

$$\text{(III)} = \lambda_z + (\text{I})_{z'},$$

$$\text{(IV)} = (\text{II})_{z'},$$

$$\text{(V)} = \lambda\lambda_{z'} - \lambda_{y'},$$

$$\text{(VI)} = \lambda\lambda_z - \lambda_y + (\text{I})\lambda_{z'} - \lambda(\text{I})_{z'} + (\text{I})_{y'} + (\text{II})(\text{V}),$$

$$\text{(VII)} = 2\lambda_z + 2\lambda_{z'}(\text{II}) - \lambda(\text{II})_{z'} + (\text{II})_{y'},$$

$$\text{(VIII)} = \lambda(\text{VI})_{z'} - (\text{VI})_{y'} + (\text{V})_y - \lambda(\text{V})_z + \lambda_{z'}(\text{VI}) - (\text{I})(\text{V})_{z'} + (\text{III})(\text{V}) - (\text{V})(\text{VII}),$$

$$\text{(IX)} = \lambda(\text{VII})_{z'} - (\text{VII})_{y'} - 2\lambda_{z'z'}(\text{I}) + 2\lambda_{yz'} - 2\lambda\lambda_{zz'} + (\text{IV})(\text{V}). \tag{4.5}$$

Also, we denote by (VI′), (IX′) the expressions (VI), (IX) without their respective last terms.

5. *Statement of Results.*—THEOREM I. *Every curve family* $\mathfrak{F}$ *which obeys the conditions* $A = 0$, $B = 0$, $C = 0$ *of Case I is an extremal family, and the*

generality of the corresponding variation problem is expressed by the symbol $\infty^{2f(3)+2f(2)}$.

It should be stated here that, in counting the arbitrary functions involved in the determination of φ when F, G are given, we omit the function $\nu(x, y, z)$ in the arbitrary exact differential $d\nu(x, y, z)$ that may always be added to φdx without changing the extremals.

THEOREM II. *In Case IIa, if the conditions*

$$\alpha = 0, \beta = 0, S = 0, K = 0 \tag{5.1}$$

are verified, then the curve family $\mathfrak{F}$ *is one of extremals, and the generality of the corresponding variation problem is* $\infty^{2f(2)}$.

THEOREM III. *In Case IIa, if the conditions* (5.1) *are not verified, but certain other conditions* (stated in our forthcoming complete paper) *are, then the given curve family* $\mathfrak{F}$ *is of extremal nature and belongs to* $\infty^{1f(2)+1f(1)}$ *different variation problems.*

THEOREM IV. *In Case IIb, if the conditions*

$$(V) = 0, (VI') = 0, (IX') = 0 \tag{5.2}$$

are satisfied, then the given curve family $\mathfrak{F}$ *can be identified with the extremals of a class of variation problems whose generality is* $\infty^{2f(2)}$.

As a preliminary to the statement of our next theorems, we introduce symbols to represent the second order determinants contained in the two-by-three matrix whose non-vanishing figures in Case III, namely:

$$\Delta_1 = BC_1 - B_1C, \Delta_2 = CA_1 - C_1A, \Delta_3 = AB_1 - A_1B. \tag{5.3}$$

Also, we let

$$D = \Delta_1\Delta_3 - \Delta_2^2. \tag{5.4}$$

Making then in the differential system, S, or (3.1), the substitutions

$$L = \rho\Delta_1, M = \rho\Delta_2, N = \rho\Delta_3, \tag{5.5}$$

we obtain a differential system of the following simple form for $\rho(x, y, z, y', z')$ as unknown function:

$$\rho_x = E_1\rho, \rho_y = E_2\rho, \rho_z = E_3\rho, \rho_{y'} = E_4\rho, \rho_{z'} = E_5\rho, \rho \neq 0; \tag{5.6}$$

where the E_i are rational expressions in the partial derivatives of F, G involving only D as denominator, and therefore existing as calculable known functions if $D \neq 0$.

THEOREM V. *In Case III, if* $D = 0$, *then the given curve family is non-extremal.*

THEOREM VI. *In Case III, if* $D \neq 0$, *then a necessary and sufficient condition for the given curve family* $\mathfrak{F}$ *to be one of extremals is that the differential*

$$E_1dx + E_2dy + E_3dz + E_4dy' + E_5dz' \tag{5.7}$$

be exact. The corresponding variation problem is essentially uniquely determined, i.e., up to a constant multiplier and an arbitrary additive exact differential, $dv(x, y, z)$.

THEOREM VII. *All curve families* $\mathfrak{F}$ *in Case IV are non-extremal.*

The preceding theorems cover all the more interesting and important cases. Certain additional minor cases are discussed in our detailed paper.

6. *Examples.*—THEOREM I: $y'' = f(z')$, $z'' = 0$, where f denotes an arbitrary function. This includes the case of the straight lines: $y'' = 0$, $z'' = 0$ treated by G. Hamel in a well-known paper.[4]

THEOREM II: The "separated case:" $y'' = F(x, y, y')$, $z'' = G(x, z, z')$, $B \neq 0$.

THEOREM III: The ∞^4 catenaries which lie in planes perpendicular to the xz-plane and the directrix of each of which coincides with the trace of its plane upon the xz-plane:

$$y'' = \frac{1 + y'^2 + z'^2}{y}, \qquad z'' = 0.$$

THEOREM IV: $y'' = z$, $z'' = 0$.

THEOREM V: $y'' = y^2 + z^2$, $z'' = 0$.

THEOREM VI: $y'' = z^2$, $z'' = y^2$. The corresponding variation problem is: $\int \left(y'z' + \frac{1}{3}y^3 + \frac{1}{3}z^3 \right) dx = \text{min.}$, up to the slight possibility of modification expressed in Theorem VI.

THEOREM VII: $y'' = y^2 + z^2$, $z'' = y$.

[1] J. Douglas, "Solution of the Inverse Problem of the Calculus of Variations," these PROCEEDINGS, **25**, 631–637 (Dec., 1939).

[2] *Bull. Amer. Math. Soc.*, **19**, 14 (1913).

[3] Subscripts attached to the roman numerals in parentheses denote partial differentiation.

[4] "Über die Geometrieen in denen die Geraden die Kürzesten sind," *Math. Annalen*, **57**, 231–264 (1903).